Reviewed Preprint
v1 • April 11, 2025
Not revised

Reviewed Preprint
v2 • March 31, 2026
Revised by authors

For correspondence:
jbai@fredhutch.org

Competing interests: No competing interests declared

Funding: See page 25

Reviewing editor: Kavita Babu, Indian Institute of Science Bangalore, India

AFD Thermosensory Neurons Mediate Tactile-Dependent Locomotion Modulation in *C. elegans*

Manuel Rosero[1,2], **Jihong Bai**[1,2]

[1]Basic Sciences Division, Fred Hutchinson Cancer Center, Seattle, United States • [2]Molecular and Cellular Biology Graduate Program, University of Washington, Seattle, United States

eLife Assessment

The manuscript presents **important** findings on how *C. elegans* can utilize distinct molecular mechanisms and circuit engagements to regulate tactile-dependent locomotory behaviours through the AFD thermosensory neuron. The authors use multiple techniques including microfluidics, genetic manipulations and single-copy rescue experiments, to provide **compelling** evidence for the role of AFD/AIB electrical synaptic connections in this behaviour. The reviewers are satisfied with the comprehensive revisions made by the authors.

https://doi.org/10.7554/eLife.106496.2.sa4

Abstract

Sensory neurons drive animal behaviors by detecting environmental stimuli and relaying information to downstream circuits. Beyond their primary roles in sensing, these neurons often form additional synaptic connections outside their main sensory modality, suggesting broader contributions to behavior modulation. Here, we uncover an unexpected role for the thermosensory neuron AFD in coupling tactile experience to locomotion modulation in *Caenorhabditis elegans*. We show that while AFD employs cGMP signaling for both thermotaxis and tactile-dependent modulation, the specific molecular components of the cGMP pathway differ between these two processes. Interestingly, disrupting the dendritic sensory apparatus of AFD, which is essential for thermotaxis, does not impair tactile-based locomotion modulation, indicating that AFD can mediate tactile-dependent behavior independently of its thermosensory apparatus. In contrast, ablating the AFD neuron eliminates tactile-dependent modulation, pointing to an essential role for AFD itself, rather than its sensory dendritic endings. Further, we find tactile-dependent modulation requires the AIB interneuron, which connects AFD to touch circuits via electrical synapses. Removing innexins expressed in AFD and AIB abolishes this modulation, while re-establishing AFD-AIB connections with engineered electrical synapses restores it. Collectively, these findings uncover a previously unrecognized function of AFD beyond thermosensation, highlighting its influence on context-dependent neuroplasticity and behavioral modulation through broader circuit connectivity.

Introduction

Adaptive behavioral responses require animals to interpret sensory signals in the context of prior experiences, enabling effective responses to changing environmental conditions. For example, rodents associate contextual cues, such as odors and colors, with rewards or punishments, leading to context-dependent adjustments in approach or avoidance behaviors [1,2]. Disruptions in the biological processes underlying this plasticity, as seen in neurological and psychiatric disorders, often result in impaired behavior modulation based on prior sensory experiences [3–7].

Recognizing the critical role of context-dependent behavioral modulation for survival and well-being, ongoing research focuses on uncovering the neuroplastic mechanisms responsible for these adaptive processes.

Studies across diverse organisms reveal that animals, regardless of nervous system complexity, integrate prior sensory experiences to shape behavior [8–15]. In the nematode *C. elegans*, which has only 302 neurons, locomotion strategies are modified by prior exposure to stimuli such as odors, touch, light, and starvation, demonstrating robust adaptive behaviors [16–23]. The wide range of adaptive behaviors, combined with the well-mapped *C. elegans* nervous system and abundant genetic tools, have empowered the discovery of fundamental circuit mechanisms and molecular pathways underlying context-dependent behavioral modulation [24–28].

The *C. elegans* sensory system comprises 60 ciliated sensory neurons specialized in detecting chemical, thermal, mechanical, and olfactory stimuli [29,30]. Each sensory neuron has a dendritic apparatus that converts specific environmental signals into neuronal activity, which drives signal flow through downstream networks of interneurons and motor neurons, ultimately shaping behavior [31–33]. Among these, AFD, a pair of bilaterally symmetric left-right neurons, serves as the primary thermosensory neurons required for thermotaxis (movement toward the a preferred temperature) [34]. The dendritic endings of AFD, enriched with microvilli, serve as the primary site for thermal detection. Even when detached from the cell body, these dendritic endings retain calcium responsiveness to temperature stimuli [35]. Moreover, genetically disrupting these sensory endings abolishes the Ca^{2+} response in AFD cell bodies to temperature changes and eliminates thermotaxis, underscoring their essential role in thermal sensing [36–38].

The second messenger cyclic guanosine monophosphate (cGMP) plays a central role in modulating AFD thermosensory activity. Temperature changes in AFD neurons trigger intracellular Ca^{2+} dynamics, with Ca^{2+} levels rising during warming and falling during cooling [35,39,40]. This response relies on cGMP synthesis mediated by the guanylyl cyclases (GCs) *gcy-8*, *gcy-18*, and *gcy-23*, which have overlapping but distinct roles. Specifically, *gcy-8* is essential for generating thermally evoked Ca^{2+} responses in AFD [41,42], whereas *gcy-18* and *gcy-23* act synergistically to sustain temperature sensing [41,43]. The cGMP produced by these cyclases activates cyclic nucleotide-gated (CNG) channels, comprised of alpha-subunits TAX-4 and beta-subunits TAX-2, resulting in increases in intracellular Ca^{2+}. Mutations in either *tax-4* or *tax-2* abolish thermally evoked Ca^{2+} responses in AFD and disrupt thermotaxis, underscoring the importance of cGMP signaling for AFD-mediated thermosensation [40].

AFD transmits thermal signals to several downstream interneurons, including AIY, AIZ, and AIB, which process this information to guide temperature-dependent behaviors. Thermotaxis in *C. elegans* encompasses three categories: movement toward warmer temperatures (thermophilic), movement toward cooler temperatures (cryophilic), and movement within a preferred temperature range (isothermal) [44,45]. Each behavior type depends on distinct AFD synaptic partners: AIY is critical for thermophilic and isothermal behaviors [46,47]; AIZ is specific for cryophilic behavior [48–50]; and AIB also supports thermophilic behavior, though its role is less critical than that of AIY [51]. These findings demonstrate the functional specificity of synaptic partners of AFD neurons in shaping distinct temperature-dependent behaviors.

In this study, we demonstrate that AFD plays a novel role in tactile-mediated, context-dependent locomotion modulation, thereby expanding its function beyond temperature sensing. The mechanisms underlying this role differ markedly from those involved in thermosensation. First, context-dependent modulation requires distinct cGMP signaling components. Second, while the microvilli-rich sensory endings of AFD are essential for thermosensation, they are dispensable for context-dependent modulation. Third, this modulation depends on mechanosensory neurons and on electrical synapses between AFD and the AIB interneuron, which connects to mechanosensory circuits. Finally, disruption of *inx-7* and *inx-10* genes, encoding gap junction protein innexins in AFD and AIB, impairs context-dependent locomotion modulation. Remarkably, restoring AFD-AIB connectivity via engineered Cx36 electrical synapses rescues this function. Collectively, our findings uncover an unconventional mechanism by which AFD mediates behavior modulation based on tactile experience.

Results

C. elegans display distinct locomotion in identical environments after exploring different physical structures

To test whether prior physical experience influences *C. elegans* behavior, we allowed worms to explore microfluidic chambers with distinct pillar designs before recording their locomotion in identical assay zones (Fig. 1A). Because the environment within the assay zone is the same across chambers, behavioral differences observed there are likely to reflect an influence of prior tactile experience. To implement this assay, we designed two microfluidic chambers that differ only in the physical structure of the exploration zone: a uniform chamber and a binary chamber (Fig. 1A). Before reaching the assay zone, worms explore surrounding areas with pillar designs that differ in size and spacing (exploration zone, Fig. 1A). This design allowed us to assess how exposure to different physical contexts impacts locomotion in an otherwise identical setting.

Worms were allowed to explore the chambers for 60 minutes before behavior was recorded in the assay zones. We found that worms in the uniform chamber assay zone exhibited locomotor behavior distinct from those in the binary chamber assay zone (Fig.1 B-F). Specifically, worms in the uniform chamber assay zone moved approximately 40% faster (Fig. 1B, F), spent ~20% less time idle (Fig. 1C, F), reversed direction ~20% less frequently (Fig. 1D, F), and turned ~30% more often (Fig. 1E, F) than worms in the binary chamber assay zone. Among the parameters measured, locomotion speed showed the most robust and reproducible modulation, establishing a stable behavioral metric for dissecting the underlying circuit and molecular mechanisms. These findings demonstrate that locomotion is shaped by past sensory experience rather than solely by immediate environmental cues.

Because worms in the binary chamber are exposed to both pillar types and remain free to move between exploration and assay zones, the behavioral differences described above could reflect exposure to a more complex physical environment rather than prior experience alone. To directly test whether locomotion is modulated by prior physical experience independently of continued access to the exploration zone, we designed microfluidic chambers in which the assay zone could be separated from the exploration zone by a removable barrier (Fig. 1–Supplement 1A). In these chambers, worms were initially allowed to explore the entire device, including exploration zones that either matched or differed from the assay zone. A barrier was then inserted to prevent worms in the assay zone from re-entering the exploration zones.

Under these conditions, locomotion immediately after barrier insertion was higher in worms that had previously explored physical settings matching the assay zone (205 ± 8 μm/s) than in worms that had explored non-matching settings (151 ± 7 μm/s; p = 0.006; Fig. 1–Supplement 1B). This difference persisted when worms were recorded 40 minutes after barrier insertion, with animals in matching chamber retaining their higher locomotion rates (218 ± 11 μm/s) compared to those in non-matching chambers (185 ± 8 μm/s; p = 0.02; Fig. 1–Supplement 1B). These findings demonstrate that prior exploration of distinct physical environments can modulate locomotion even when worms are prevented from returning to those environments, supporting a role for prior physical experience independent of ongoing sensory input.

Guanylyl cyclase gene *gcy-18* is required for context-dependent locomotion modulation in chambers

To identify mechanisms underlying context-dependent locomotion adjustments, we employed a previously reported preference assay that uses microfluidic arenas to assess the ability of worms to select a preferred space [52]. Because worms must adjust their locomotion based on their surroundings to remain within a preferred area, we hypothesized that mutations abolishing this preference would reveal key mechanisms underlying context-dependent adjustments in the

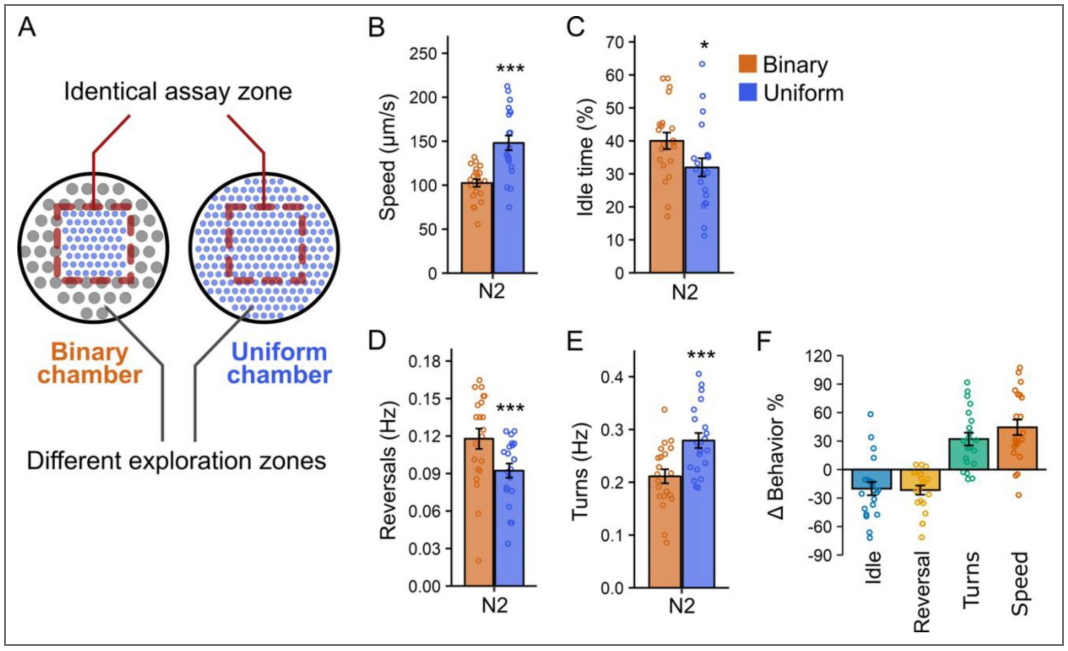

Figure 1. ***C. elegans*** **displays distinct locomotion in identical environments after exploring different surrounding areas.**

(A) Schematic of two microfluidic chamber designs: uniform and binary. Both chambers contain an identical assay area (red dashed-line boxes) where locomotion was analyzed, while the surrounding exploration zones differ in PDMS pillar arrangement. (B-E) Quantification of locomotion in the assay area after 1 hour of exploration. Data from binary chambers (n = 21) are shown in orange and from uniform (n = 21) chambers in blue. Shown are (B) locomotion speed, (C) percentage of time spent idle, (D) reversal frequency, and (E) turning frequency. Statistical significance was determined using an unpaired Student's t-test (***p < 0.001, *p < 0.05). Mean ± SEM; each point represents the mean behavioral value of all worms within one chamber. (F) Percent change in each locomotion metric (speed, idle time, reversal frequency, and turning frequency), calculated from panels B-E and normalized to the mean value in binary chambers. Mean ± SEM; each point represents the mean behavioral value of all worms within one chamber.

uniform and binary chambers. Accordingly, we screened for mutant worms that failed to choose their preferred area, aiming to identify the genetic mechanisms mediating locomotion adjustments in response to different physical structures.

Given the significant role of cGMP in neuronal plasticity and behavior modulation, we performed a small-scale genetic screen using loss-of-function mutants for 24 genes encoding guanylyl cyclases (GCs), the enzymes responsible for cGMP synthesis. Using the preference assay, we identified two putative null mutants, *gcy-18(gk423024)* and *gcy-12(gk142661),* that displayed significant defects in spatial preference (Fig. 2–Supplement 1A). We then compared the locomotion of *gcy-18* and *gcy-12* mutants in both uniform and binary chambers. *gcy-12* mutant worms exhibited normal speed adjustment compared to wild type (Δspeed: *gcy-12*: 24 ± 5% vs. N2: 35 ± 7%, p = 0.27, Fig. 2–Supplement 1B), indicating that *gcy-12* is not required for locomotion modulation. In contrast, *gcy-18(gk423024)* mutants failed to execute context-dependent speed adjustment (Δspeed *gcy-18*: 3 ± 5% vs. N2: 35 ± 7%; p = 0.0013; Fig. 2A). A second allele, *gcy-18(nj38),* similarly showed significantly reduced Δspeed (11 ± 2%; p =0.011 compared to wild type; Fig. 2A). Together, these results indicate that *gcy-18* is required for context-dependent behavioral adjustment.

To confirm that the defects observed in *gcy-18* mutants were not due to background artifacts, we introduced a single-copy *gcy-18* transgene driven by the *gcy-18* promoter into *gcy-18(gk423024)* mutants. Expression of this transgene restored locomotion adjustments to near wild type levels (Δspeed: *gcy-18p::gcy-18*: 28 ± 6% vs. N2: 35 ± 7%, p = 0.8, Fig. 2B), confirming that loss of *gcy-18* underlies the observed behavioral defects. The identification of *gcy-18* was particularly intriguing, as its expression is restricted to a single pair of neurons, the thermosensory AFDs. Given that our assay chambers lacked thermal gradients, these findings suggest a previously unrecognized role for *gcy-18* and AFD neurons in mediating locomotion adjustments based on prior exploration of physical environments.

To further investigate the role of AFD-specific guanylyl cyclases in context-dependent locomotion modulation, we examined *gcy-8*, which is essential for generating thermally evoked Ca^{2+} responses in AFD [41,42]. In thermal responses, disrupting *gcy-8* alone is sufficient to impair AFD function, whereas disruption of *gcy-18* alone does not [41,43], indicating the critical role of GCY-8 in AFD thermosensation. If *gcy-18* influenced behavioral adjustment in microfluidic chambers solely through its role in thermosensation, we would expect that a loss-of-function mutation in *gcy-8* would have a similar or even more disruptive impact on locomotion modulation. However, *gcy-8* mutant worms exhibit little change in their ability to adjust locomotion speed, with Δspeed values similar to that observed in wild type worms (Δspeed: *gcy-8*: 29 ± 7% vs. N2: 35 ± 7%; p = 0.96; Fig. 2C). These results indicate that while *gcy-8* is critical for thermosensation, its mutation does not affect context-dependent locomotion modulation, suggesting that independent cGMP signaling mechanisms govern AFD neuronal activity in thermosensation and context-dependent behavior in microfluidic chambers (Fig. 2D).

Distinct CNG channels mediate context-dependent locomotion modulation and thermosensation

The role of guanylyl cyclase in cGMP synthesis prompted us to investigate whether cyclic nucleotide-gated (CNG) channels are involved in context-dependent locomotion modulation. CNG channels, composed of α and β subunits, open upon binding cyclic nucleotides (*e.g.*, cGMP and cAMP), allowing Ca^{2+} influx [53–56] to control signal transduction and neural plasticity across species [57–64] (Fig. 3A). In *C. elegans*, mutations in either the *tax-4* or *tax-2* genes, which encode the α and β subunits of CNG channels respectively, impair thermotaxis behavior [47,65] and eliminates AFD responses to temperature changes [40,66]. To determine their role in context-dependent locomotion modulation, we examined *tax-4(p678)* and *tax-2(p694)* mutant worms using our microfluidic chamber assay.

We found that *tax*-2 is essential for context-dependent locomotion modulation, as *tax-2* mutants did not exhibit differences in speed between chamber types (Fig. 3B, C). In contrast, *tax-4* mutants displayed an enhanced locomotion adjustment compared to wild type worms (Δspeed:

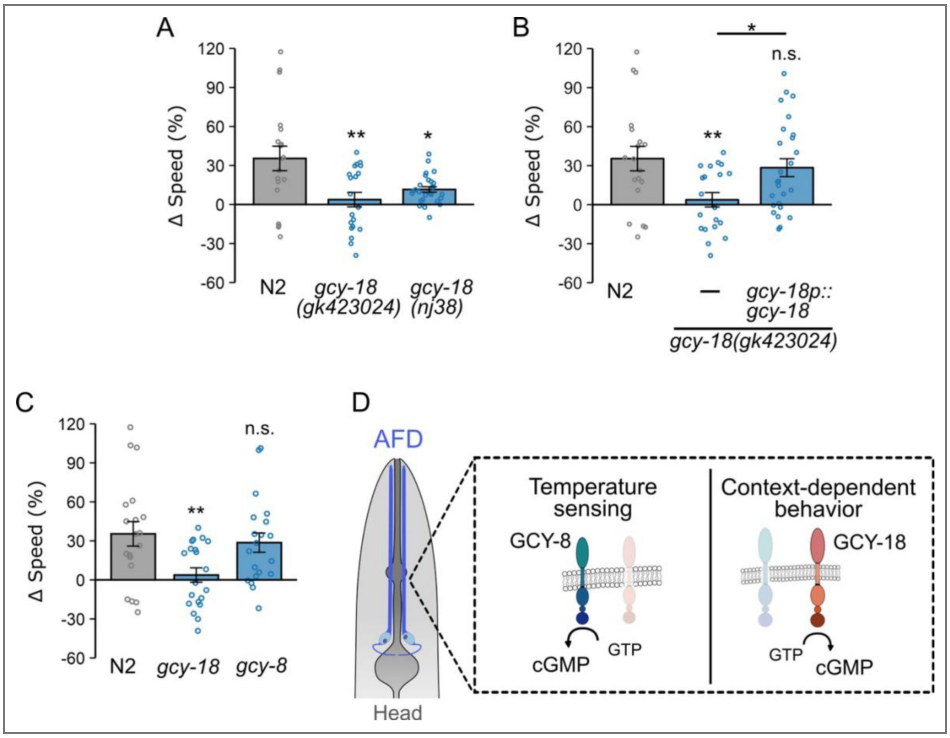

Figure 2. Guanylate cyclase gene *gcy-18* functions in AFD to mediate context-dependent locomotion modulation.

(A) Difference in locomotion speed (Δspeed) between uniform and binary chambers of wild type N2 (uniform: n = 19; binary: n = 20), *gcy-18(gk423024)* mutant (uniform: *n* = 20; binary: n = 28), and *gcy-18(nj38) mutant* (uniform: *n* = 27, binary: n = 27). ΔSpeed was calculated as the percent change in locomotion speed in uniform chambers, relative to the mean speed measured in binary chambers (see Methods). Mutant worms lacking *gcy-18* failed to demonstrate context-dependent locomotion adjustments in locomotion speed, as indicated by a low Δspeed value. (B) Δspeed of wild type, *gcy-18* mutants, and *gcy-18* mutant worms carrying a single-copy transgene expressing *gcy-18* under the control of the *gcy-18* promoter. Expression of *gcy-18p::gcy-18* restored Δspeed (uniform: n= 26; binary: n = 24). (C) Locomotion speed adjustment of N2, *gcy-18* mutants, and *gcy-8* mutant worms (uniform: n = 20, binary: n = 18). Disruption of *gcy-8* does not impair context-dependent locomotion modulation. (D) Schematic illustrating the distinct roles of guanylate cyclase genes in AFD sensory neurons: *gcy-8* is required for thermosensation but not for context-dependent locomotion modulation, whereas *gcy-18* is essential for context-dependent locomotion modulation and plays only a modest role in thermosensation. Data are presented as mean ± SEM. Each data point represents the mean behavior of worms within a single chamber. Asterisks above bars indicate statistical significance compared to wild type, whereas asterisks above horizontal black lines indicate statistical significance between mutant strains. Statistical significance was determined using one-way ANOVA followed by a Tukey-Kramer post hoc test (n.s.: $p > 0.05$; *: $p < 0.05$; **: $p < 0.01$).

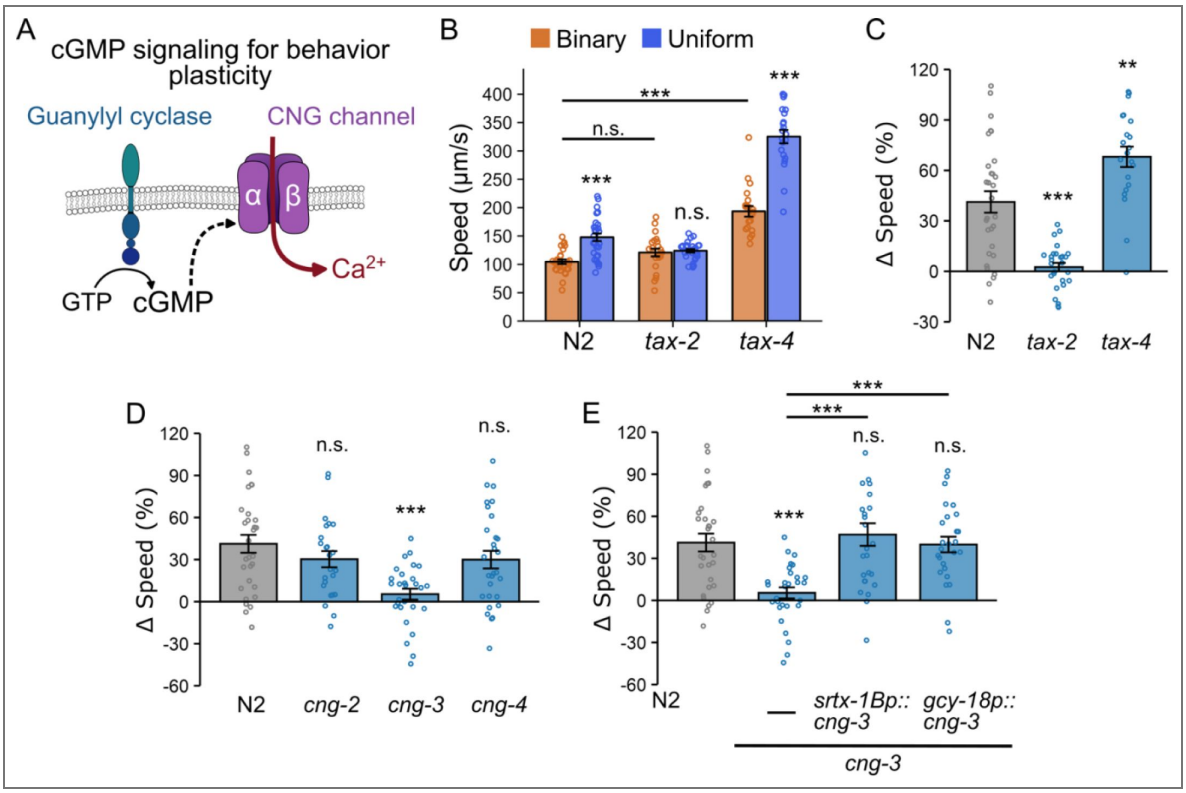

Figure 3. Cyclic nucleotide-gated (CNG) channel subunits TAX-2 and CNG-3 are required for locomotion modulation, but TAX-4 is not.

(A) Schematic representation of CNG channel function. CNG channels are activated by cyclic nucleotides (such as cGMP) and mediate Ca^{2+} influx, thereby influencing neuronal activity and animal behavior. (B) Locomotion speed (μm/s) of N2 (uniform: n = 30; binary: n = 29), *tax-2* (uniform: n = 27; binary: n = 22), and *tax-4* (uniform: n = 21; binary: n = 21) mutant worms in binary (orange) and uniform (blue) chambers. The *tax-2* mutants exhibit identical locomotion rates in both chamber types, whereas worms lacking *tax-4* display accelerated basal locomotion while still preserving context-dependent locomotion modulation. Asterisks above blue bars indicate statistically significant differences in locomotion speed between uniform and binary chambers (unpaired Student's *t*-test). Asterisks above horizontal black lines indicate statistically significant differences in basal speed, defined as speed of worms in the binary chamber, between N2 and *tax-4* mutants (one-way ANOVA followed by a Tukey-Kramer post hoc test; *n.s.*: $p > 0.05$; ***: $p < 0.001$). (C) Speed differences (Δspeed) for N2, *tax-2* mutant, and *tax-4* mutant worms. The *tax-2* mutants failed to modulate locomotion rates in a context-dependent manner, whereas *tax-4* mutations enhanced modulation. (D) Assessment of *cng-2* (uniform: n = 24; binary: n = 22), *cng-3* (uniform: n = 29; binary: n = 28), and *cng-4* (uniform: n = 24; binary: n = 29) roles in locomotion adjustments. The *cng-3* mutation abolishes locomotion modulation. (E) Single-copy transgenes expressing *cng-3* cDNA under two AFD-specific promoters, *srtx-1bp* (uniform: n = 26; binary: n = 22) and *gcy-18p* (uniform: n = 26; binary: n = 25), restore context-dependent locomotion adjustments. Data are presented as mean ± SEM. Each data point represents the mean behavior of worms within a single chamber. Asterisks denote statistical significance versus wild type (above bars) or between mutant strains (above horizontal black lines). Δspeed comparisons across strains (panels C-E) were determined using one-way ANOVA followed by Tukey-Kramer post hoc tests (*: $p < 0.05$; **: $p < 0.01$, and ***: $p < 0.001$).

tax-4: 68 ± 6% vs. N2: 41± 6%; p = 0.002; Fig. 3C), a striking difference from the lack of speed changes seen in *tax-2* mutants (Δspeed: *tax-2*: 2 ± 2%; p < 0.0001 compared to wild type). We examined the locomotion speed of mutant worms in the binary chambers, which we refer to as the basal speed because wild type worms consistently move slowest in this environment. We found *tax-4* mutants showed significantly higher basal speed than the wild type (*tax-4:* 193 ± 9 μm/s vs. N2: 104 ± 4 μm/s, p < 0.0001; Fig. 3B), indicating that *tax-4* mutants can still adjust locomotion speed based on prior experience even when basal locomotion is accelerated.

To further examine how basal locomotion influences context-dependent modulation, we took advantage of the fact that worm locomotion rates are sensitive to environmental temperature [67,68]. We examined the relationship between temperature-induced changes in basal locomotion and locomotion modulation based on prior experience of physical surroundings. Wild type worms cultivated at either 23°C or 17°C and then transferred to 20°C exhibited significantly changes in basal locomotion speed. Despite changes in basal speed, the extent of locomotion modulation in the chambers was largely unaffected (Fig.3–Supplement 1A). Specifically, locomotion speed was positively correlated with temperature shifts in both chambers (binary chambers: r = 0.52, p < 0.0001; uniform chambers: r = 0.48, p < 0.0001; Fig.3–Supplement 1B), whereas no significant correlation was observed between temperature and Δspeed (r = −0.03, p = 0.22; Fig.3—Supplement 1C), supporting the notion that basal locomotion speed and context-dependent modulation are regulated independently.

Together, these observations indicate that TAX-2 is required for integrating prior experience into locomotion modulation, whereas TAX-4 primarily regulates overall locomotion level. Although both pathways engaging cGMP signaling, their distinct phenotypes suggest separate regulatory mechanisms for basal locomotion and context-dependent adjustments.

Given that four other genes (*cng-1*, *cng-2*, *cng-3* and *cng-4*) are predicted to encode CNG channels in *C. elegans,* we investigated their role in locomotion modulation in microfluidic chambers [69]. Due to abnormal development in *cng-1* mutants, we were unable to assess their locomotion; however, we were able to evaluate mutants of the other three genes. We found that *cng-3(gk541751)* mutant worms showed significantly decreased speed modulation compared to wild type (Δspeed: *cng-3:* 5 ± 4%, p = 0.0002; Fig. 3D), while *cng-2(tm4267)* and *cng-4(gk195496)* mutants exhibited normal modulation comparable to wild type worms (p = 0.54 and p = 4.47 respectively; Fig. 3D). The identification of CNG-3 was particularly intriguing, as recent studies suggest that it mediates changes in AFD neuronal activity based on prior temperature experiences [70,71], indicating that CNG-3 contributes to neural plasticity rather than direct stimulus detection. Our results further support this view by showing that CNG-3 plays a broader role in locomotion modulation in environments lacking thermal gradients, which suggests its involvement in neuronal plasticity beyond the thermosensory modality.

Next, we determined whether AFD is the site where CNG-3 functions in context-dependent locomotion modulation. To do so, we introduced single-copy transgenes expressing *cng-3* cDNA under the control of two AFD-specific promoters, *srtx-1Bp* and *gcy-18p*, into *cng-3(gk541751)* mutant worms. Regardless of the promoter used, AFD-specific expression of *cng-3* restored the locomotion speed modulation to levels comparable to wild type (Δspeed: *srx-1Bp::cng-3*: 47 ± 8%; p < 0.0001 compared to *cng-3* mutant, p = 0.91 compared to wild type; and *gcy-18p::cng-3:* 40 ± 6%, p = 0.0007 compared to *cng-3* mutant, p = 0.99 compared to wild type; Fig. 3E). These results indicate that AFD neurons are the site of action for CNG-3 in mediating context-dependent locomotion modulation. Together, our findings reveal a role for AFD beyond thermosensation and show that components of a cGMP signaling pathway enable AFD to modulate locomotion in an experience-dependent manner.

AFD sensory microvilli are dispensable for locomotion modulation, but AFD neurons are required

The finding that GCY-18 and CNG-3 in AFD neurons are required for context-dependent locomotion prompted us to test whether the AFD thermosensory apparatus is also necessary for this function. This apparatus consists of sensory microvilli at the tip of the AFD dendrite (Fig. 4A) and is essential for temperature sensing and thermotaxis [36,38]. For example, mutations in the *kcc-3* gene, which encodes a K^+/Cl^- cotransporter in the amphid sheath glia, disrupt microvilli formation and significantly impair thermotaxis toward the cultivation temperature [37].

Despite this disruption, locomotion modulation based on experience of physical settings remained intact in *kcc-3(ok228)* mutant worms compared to wild type (Δspeed: *kcc-3*: 33 ± 4% vs. N2: 42 ± 7%, p = 0.28; Fig. 4B, C). *kcc-3* mutants also displayed elevated basal locomotion rates (basal speed: *kcc-3:* 174 ± 8 μm/s vs. N2: 115 ± 7 μm/s, p < 0.0001; Fig. 4B), similar to what we observed in *tax-4* mutants. This supports our earlier finding that overall locomotion rate does not necessarily correlate with context-dependent modulation.

To further test whether AFD sensory endings are required for context-dependent locomotion modulation, we examined *ttx-1(767)* mutant worms, which completely lack AFD microvilli and exhibit more severe thermotaxis defects than *kcc-3* mutants [38]. Despite the loss of sensory microvilli, *ttx-1* mutants retained the ability to modulate locomotion in microfluidic chambers. The extent of modulation was modestly reduced and more variable compared to wild type animals (Δspeed: *ttx-1*: 29 ± 10% vs. N2: 42 ± 7%, p = 0.29, Fig. 4D). Because *ttx-1* mutations disrupt the expression of multiple AFD genes, including components of the cGMP signaling pathway [72], this increased variability may reflect broader perturbations in AFD function. Nonetheless, these results indicate that AFD sensory microvilli are not strictly required for context-dependent locomotion modulation.

Given that *gcy-18* is required for context-dependent locomotion modulation and that GCY-18 localizes to the distal dendrite of AFD, we next examined how disruption of sensory microvilli affects its localization in AFD. We used a split-GFP strategy to visualize endogenous GCY-18 [73]. A tandem array of seven GFP11 β-strands (GFP11x7) was inserted at the C-terminus of GCY-18 using CRISPR-Cas9. When complemented with GFP1-10, GCY-18::GFP11x7 fluorescence was strongly enriched at the AFD sensory microvilli near the nose (Fig. 4–Supplement 1A-A"), consistent with previous reports [42,74,75]. In addition, weaker but reproducible GCY-18 signal was detected near the AFD soma and axon (Fig. 4–Supplement 1A"'). Importantly, in *kcc-3*, which exhibit disrupted sensory microvilli, and *ttx-1* mutants, which lack sensory microvilli, GCY-18 remained localized to the distal dendrite and was still detectable near the soma and axon (Fig. 4–Supplement 1B-B"' and 1C-C"'). Although these experiments do not identify the precise subcellular site at which GCY-18 acts, they show that disruption or loss of sensory microvilli does not substantially alter GCY-18 localization within AFD.

We next asked whether AFD neurons themselves are required for this behavior. Using a published strain expressing caspase under the AFD-specific *gcy-8* promoter [76], we found that AFD-ablated worms completely lost the ability to adjust locomotion in microfluidic chambers. These animals showed no detectable differences between uniform and binary chambers in locomotion speed, idle time, or turning frequency (Fig. 4E). Together, these results indicate that while AFD sensory microvilli are dispensable for context-dependent locomotion modulation, the AFD neurons themselves are essential.

Building on our finding that locomotion modulation can be driven by prior physical experience even after worms are prevented from re-entering the exploration zones, we next tested whether AFD is required for this modulation using chambers in which the exploration and assay zones were separated by a removable barrier (Fig. 1–Supplement 1A). Under these conditions, locomotion modulation was significantly reduced in AFD-ablated worms (Δspeed: -AFD = 1 ± 6% vs. N2 = 23 ± 7%; p = 0.036; Fig. 4–Supplement 2A). Similarly, *gcy-18* mutants showed defective

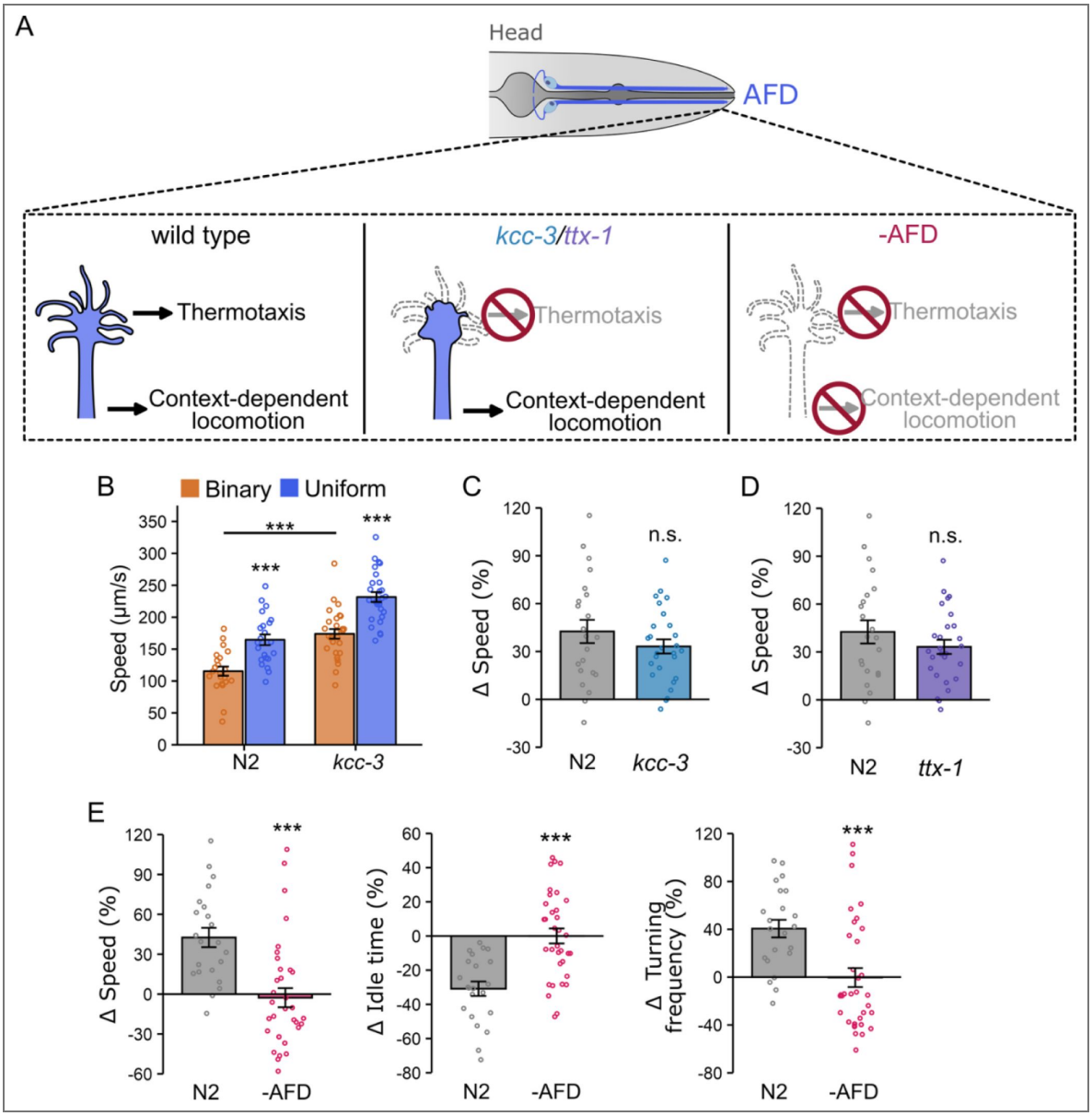

Figure 4. AFD, but not its sensory endings, is required for context-dependent locomotion modulation.

(A) Schematic representation of AFD function in temperature sensing and locomotion modulation. AFD sensory endings are essential for thermosensation but dispensable for context-dependent locomotion modulation. (B) Locomotion speed (μm/s) of wild type N2 (uniform: n = 22; binary: n = 22) and *kcc-3* (uniform: n = 27; binary: n = 27) mutant worms in the binary (orange) and uniform (blue) chambers. The *kcc-3* mutants preserve context-dependent locomotion modulation while exhibiting increased basal locomotion rates. Asterisks above blue bars indicate significant differences between uniform and binary chambers (unpaired Student's *t*-test). Basal speed differences in the binary chambers were determined using one-way ANOVA followed by a Tukey–Kramer post hoc tests (***: $p < 0.001$). (C) Δspeed of N2 and *kcc-3* mutant worms, and (D) Δspeed of N2 (uniform: n = 22; binary: n = 22) and *ttx-1* (uniform: n = 27; binary: n = 27)mutant worms. Context-dependent locomotion modulation remains in *kcc-3* and *ttx-1* mutant worms, although they abolish the AFD thermosensory function. (E) Ablation of AFD eliminates the context-dependent modulation of speed, idle time, and turning frequency (uniform: n = 34; binary: n = 36). Data are presented as mean ± SEM. Each data point represents the mean behavior of worms within a single chamber. Asterisks indicate statistical significance compared to wild type. Δspeed across strains (panels C-E) was analyzed by one-way ANOVA followed by Tukey-Kramer post hoc tests (n.s.: $p > 0.05$, and ***: $p < 0.001$).

locomotion modulation (Δspeed: *gcy-18* = -1 ± 8% vs. N2 = 23 ± 7%; p = 0.034; Fig. 4–Supplement 2A). These results indicate that AFD and *gcy-18* are required to generate locomotion modulation in response to recent physical experience.

Finally, to determine whether the modulation defects observed in *gcy-18* mutants and AFD-ablated worms could be attributed to developmental abnormalities or gross motor impairments, we measured locomotion speed and body length on standard NGM plates. Both day-1 adult AFD-ablated worms (speed: 281 ± 10 μm/s; p = 0.33; body length: 1.12 ± 0.01 mm; p = 0.76) and *gcy-18* mutants (speed: 291 ± 13 μm/s; p = 0.22; body length: 1.15 ± 0.02 mm; p = 0.86) showed locomotion speeds and body lengths comparable to wild type controls (speed: 252 ± 30 μm/s; body length: 1.14 ± 0.02 mm; Fig. 4–Supplement 2B, C). These results indicate that the loss of context-dependent locomotion modulation is not due to developmental defects or gross impairments in locomotion.

Context-dependent locomotion modulation requires the MEC-10 mechanosensory channel subunit

Having established that AFD integrates prior physical experience independent of its thermosensory apparatus, we next asked whether direct mechanosensory input is required for context-dependent locomotion modulation. The *mec-10* gene encodes an amiloride-sensitive Na^+ channel protein required for sensing body touch. Mutations in *mec-10* disrupt mechanotransduction channels in the worms, impairing touch sensitivity [77,78]. We found that *mec-10(tm1552)* mutants failed to display locomotion adjustment compared to wild type worms (Δspeed: *mec-10*: 5 ± 4% vs. N2: 33 ± 6%, p = 0.0003; Fig. 5A). These results show that *mec-10* is crucial for context-dependent locomotion modulation, supporting the hypothesis that locomotion is modulated depending on the worm's tactile experience.

The *mec-10* gene is expressed in several mechanosensory neurons, including the six touch receptor neurons (TRNs) and the polymodal nociceptors FLP and PVD [77,79]. To determine which neurons are required for tactile-dependent locomotion modulation, we expressed *mec-10* cDNA under cell-specific promoters: *mec-18p* (TRNs) [80], *egl-44p* (FLP) [81], or *mec-10p* (TRNs, FLP, and PVD) [79]. Expression in either FLP or TRNs alone did not restore modulation, as worms carrying *egl-44p::mec-10* (Δspeed: −11 ± 4%) or *mec-18p::mec-10* (Δspeed: −13 ± 4%) transgenes showed significantly reduced Δspeed compared to wild type (Δspeed: N2: 33 ± 6%; p < 0.0001 for both; Fig. 5A). By contrast, *mec-10* co-expression in both FLP and TRNs (Δspeed: 16 ± 4%), or expression from the *mec-10* promoter (Δspeed: 23 ± 4%), restored Δspeed to wild type levels (p = 0.20 and p = 0.57, respectively; Fig. 5A). These findings indicate that *mec-10* expression across multiple mechanosensory neuron types is required for context-dependent locomotion modulation. It is also worth noting that, while both tactile-dependent locomotion modulation and previously reported spatial preference require FLP, only the former depends on TRNs. Together, these findings suggest that distinct subsets of mechanosensory neurons differentially contribute to behaviors shaped by tactile experience.

AIB interneurons are crucial for tactile-dependent behavioral plasticity

Touch-sensitive neurons that express *mec-10*, including TRNs, FLP, and PVD, do not form direct synapses with AFD, suggesting that tactile information is relayed through intermediary neurons. Because the interneuron AIB receives synaptic input from FLP and forms electrical synapses with AFD, we hypothesized that AIB could serve as a conduit for mechanosensory signals to reach AFD. To test whether AIB is required for tactile-dependent modulation, we examined locomotion in worms with genetically ablated AIB neurons using *npr-9p::caspase* expression [82]. AIB-ablated worms failed to adjust locomotion speed, showing a near-complete loss of modulation (Δspeed: −1 ± 5%) compared to wild type (30 ± 8%, p = 0.001, Fig. 5B). These results demonstrate that AIB is required for AFD-mediated tactile-dependent locomotion modulation. However, because *mec-10*-expressing TRNs are also required, additional pathways beyond AIB likely contribute to

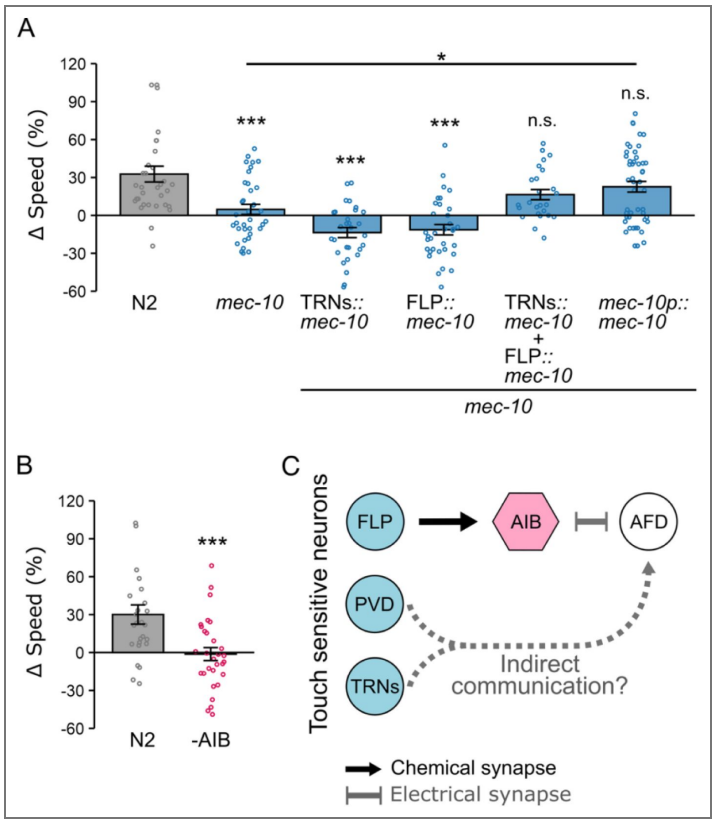

Figure 5. Context-dependent locomotion adjustments require the mechanosensory channel subunit MEC-10 and the interneuron AIB.

(A) Δspeed of wild type (uniform: n = 26; binary n = 22), *mec-10* mutants (uniform: n = 30; binary n = 21), and *mec-10* mutants expressing *mec-10* cDNA under cell-specific promoters: *mec-18p* (TRNs; uniform: n = 29; binary n = 25), *egl-44p* (FLP; uniform: n = 27; binary n = 34), or *mec-10p* (TRNs, FLP, and PVD; uniform: n = 32; binary n = 26). (B) Δspeed of wild type and AIB-ablated worms (uniform: n = 30; binary n = 30). AIB ablation abolishes speed modulation. Data are shown as mean ± SEM; each data point represents the average speed of worms in a single chamber. Asterisks indicate statistical significance compared to wild type (one-way ANOVA followed by Tukey-Kramer post hoc tests; ***p < 0.001). (C) Schematic illustrating a circuit framework connecting *mec-10* expressing neurons, AIB, and AFD in tactile-dependent modulation of locomotion.

transmitting tactile information to AFD, potentially involving indirect synaptic connections through other interneurons or long-distance signaling via neuropeptides or other modulators (Fig. 5C).

Mutations in *innexin* genes disrupt tactile-dependent modulation

Electrical synapses between AIB and AFD neurons in *C. elegans* are formed by gap junction proteins known as innexins [83]. If electrical coupling between AIB and AFD contributes to tactile-dependent locomotion modulation, then disruption of innexin genes should impair locomotion adjustments in microfluidic chambers. To test this, we examined loss-of-function mutants of several innexin genes. *C. elegans* possesses 25 innexin genes [84,85]. Single-cell RNA-seq data from the CeNGEN database [86] indicate that three genes (*inx-4, inx-10,* and *inx-19)* are expressed in AFD, one (*inx-1)* is expressed in AIB, and one (*inx-7*) is expressed in both. We found that *inx-4*, *inx-7*, and *inx-10* mutants exhibited a partial but significant reduction in locomotion modulation compared to wild type worms (Δspeed: N2: 45 ± 7%; *inx-4*: 23 ± 5%, p = 0.037; *inx-7*: 21 ± 5%, p = 0.013; *inx-10*: 16 ± 3%, p = 0.0007; Fig. 6A). Mutations in *inx-1* also reduced Δspeed values, although the effect did not reach statistical significance (Δspeed: *inx-1:* 25 ± 6%, p = 0.076), whereas *inx-19* mutations had little impact on speed modulation (*inx-19:* 32 ± 5%, p = 0.51, vs. wild type; Fig. 6A). Furthermore, *inx-7; inx-10* double mutants exhibited a more pronounced reduction in Δspeed compared to single mutants (Δspeed: *inx-7; inx-10* double mutant: 6 ± 5%; p = 0.032 compared to *inx-7* single mutant; Fig. 6B). Together, these findings suggest that multiple innexin genes act redundantly to support tactile-dependent locomotion modulation.

Targeted electrical coupling between AFD and AIB restores tactile-dependent modulation

We next tested whether restoring *inx-10* specifically in AFD would be sufficient to rescue the behavioral defect. Using the AFD-specific *srtx-1b* promoter, we expressed *inx-10* cDNA in *inx-10* mutant worms. These transgenic animals displayed significantly improved locomotion modulation (Δspeed: 42 ± 5%) compared to non-transgenic *inx-10* mutants (15 ± 4%; p = 0.018; Fig. 6D), indicating that *inx-10* expression in AFD alone is sufficient to restore function.

To directly test whether restoring the electrical connection between AFD and AIB could rescue modulation in innexin mutants, we expressed the mammalian gap junction protein Cx36 [87–90] in both AFD (*srtx-1Bp*) and AIB (*inx-1p*) neurons in *inx-7; inx-10* double mutants (Fig. 6C). Cx36 expression significantly improved locomotion modulation, restoring Δspeed from 7 ± 4% to 35 ± 8% (p = 0.0035; Fig. 6D). These results demonstrate that although innexin mutations disrupt connectivity across multiple neurons, restoring a single targeted electrical connection between AFD and AIB is sufficient to rescue tactile-dependent locomotion modulation, identifying the AIB-AFD electrical synapse as a critical circuit element for tactile-dependent behavioral control.

Discussion

Our study reveals that the thermosensory AFD neuron plays an unexpected role in coupling tactile experiences to locomotion modulation in *C. elegans*. We show that: 1) *C. elegans* exhibit distinct locomotion patterns in identical environments, influenced by prior tactile experiences; 2) tactile-dependent behavior modulation requires the AFD neuron but not its thermosensory dendritic endings; 3) thermotaxis and tactile-dependent locomotion modulation rely on distinct sets of cGMP signaling proteins and CNG channel subunits; 4) the AIB interneuron, which connects AFD to mechanosensory circuits, is essential for tactile modulation; and 5) electrical synapses between AFD and AIB are critical for this process. Below, we discuss the implications of these findings.

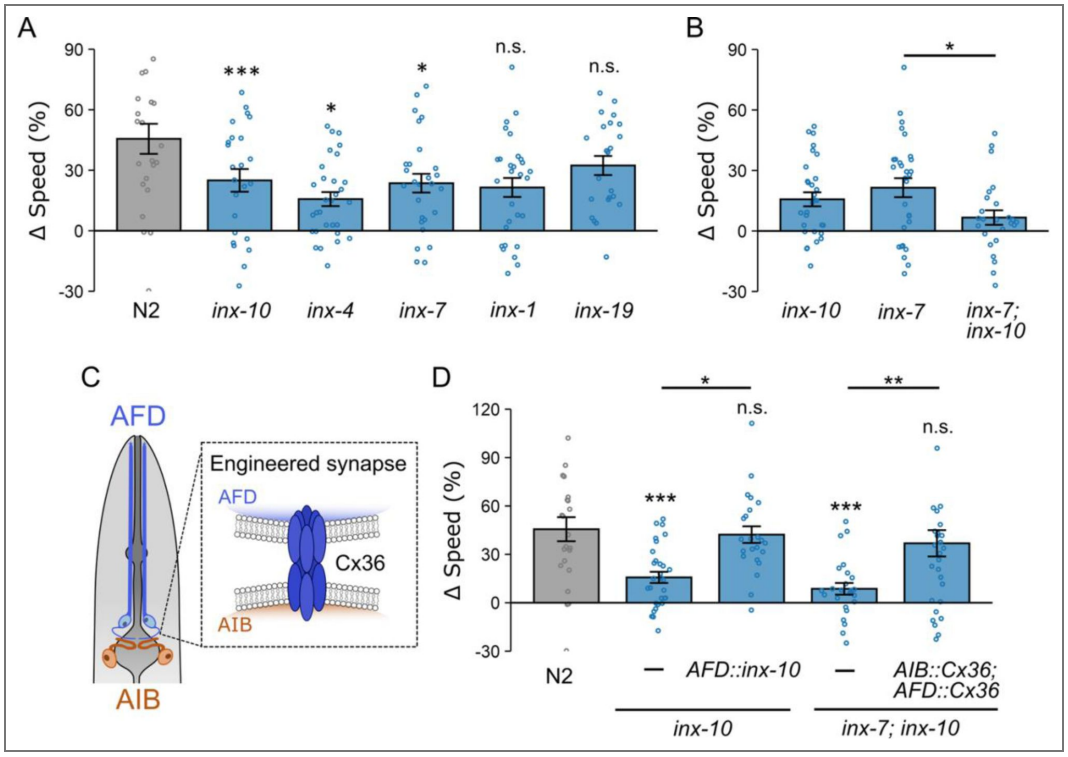

Figure 6. Tactile-dependent locomotion modulation is disrupted in mutant worms lacking gap junction genes and is restored by engineered Cx36 electrical synapses linking AFD and AIB.

(A) Speed differences (Δspeed) for wild type worms (uniform: n = 23; binary: n = 25) and *inx-1* (uniform: n = 24,; binary: n = 24), *inx-4* (uniform: n = 27; binary: n = 26), *inx-7* (uniform: n = 29; binary: n= 30), *inx-10* (uniform: n = 30; binary: n = 29), *inx-19* (uniform: n = 23; binary: n = 24) mutants. (B) Speed differences for *inx-7; inx-10* double mutants (uniform: n = 25; binary: n = 27). (C) Schematic illustrating engineered electrical synapses formed by Cx36 when expressed in adjacent neurons. (D) AFD-specific expression of *inx-10* cDNA restored tactile-dependent locomotion modulation in *inx-10* mutant worms (*srtx-1bp*; uniform: n = 23; binary: n = 24). Expression of Cx36 in both AFD (*srtx-1bp*) and AIB (*inx-1p*) similarly restored modulation in *inx-7; inx-10* double mutants (uniform: n = 30; binary: n = 28). Data are presented as mean ± SEM. Asterisks denote statistical significance versus wild type (above bars) or between indicated genotypes (above horizontal black lines). Each data point represents the mean behavior of worms within a single chamber. Statistical significance was determined using one-way ANOVA followed by Tukey-Kramer post hoc tests (*: $p < 0.05$; **: $p < 0.01$, and ***: $p < 0.001$).

A thermosensation-independent role for AFD in tactile-dependent behavior modulation

Our findings highlight the remarkable versatility of sensory neurons in shaping behaviors beyond their primary functions. This supports the emerging view that sensory neurons have multifaceted roles in circuit modulation, extending well beyond canonical sensory activities. Such complexity is encoded at multiple levels within neural circuits. In *C. elegans*, for instance, the ASH neuron drives avoidance responses to various noxious stimuli, including hyperosmolarity, nose touch, and volatile repellents, demonstrating polymodal functionality [91–94]. Similarly, the olfactory receptor neuron AWC exhibits stochastic responses to temperature, introducing variability that enhances the flexibility and reliability of thermotactic behavior [95–97]. In contrast to these examples, the role of AFD in tactile-dependent plasticity does not rely on its sensory endings but is mediated through synaptic connectivity. This reveals an unexpected mechanism by which AFD influences context-dependent behavioral plasticity via network-level interactions rather than direct sensory activity.

Distinct cGMP signaling pathways in AFD mediate sensation and plasticity

Our data indicates that the CNG channel α subunits TAX-4 and CNG-3 play distinct roles in AFD function. Although TAX-4 is essential for AFD to detect temperature and generate thermally evoked responses [40], it is dispensable for tactile-dependent locomotion modulation. By contrast, CNG-3, which is not required for temperature sensing [70], is crucial for tactile-dependent locomotion modulation. Consistent with a broader role in sensory plasticity, CNG-3 is required in AWC neurons for short-term odor adaptation [98] and in AFD for adjusting temperature thresholds based on prior thermal experiences [70]. Our demonstration that CNG-3 is essential for tactile-dependent locomotion modulation further supports the view that CNG-3 enables context-dependent behavioral plasticity rather than directly mediating stimulus detection.

CNG channels are heteromeric complexes composed of both α and β subunits. Our data, along with previous work, show that TAX-2, the CNG β subunit in *C. elegans*, is required for both tactile-dependent locomotion modulation and thermotransduction [40]. Interestingly, TAX-4, the canonical α partner of TAX-2, is not required for tactile-dependent modulation. This suggests that TAX-2 may support experience-dependent neural plasticity either on its own or by pairing with alternative α subunits such as CNG-3. This type of functional specialization is reminiscent of photoreceptor neurons, where the composition and ratio of CNG channel subunits determine light sensitivity and enable contrast detection under varying light intensities [99–101]. It is worth noting that the *tax-2(p694)* mutation affects *tax-2* expression in four neurons (AFD, BAG, ASE, and ADE) [102]. Moreover, the strong convergence of functional and circuit-level evidence, including the requirement for GCY-18, the rescue of CNG-3 function in AFD, and role of AIB–AFD coupling, points to AFD as the most likely site of TAX-2 function in tactile-dependent locomotion modulation.

In addition to the diversity of CNG channels, guanylyl cyclases in AFD also exhibit functional specificity. For example, mutations in *gcy-18* alone significantly disrupt tactile-dependent locomotion modulation without substantially affecting temperature sensing [41,43], whereas *gcy-8* is essential for generating thermally evoked Ca^{2+} responses [41,42] yet appears dispensable for tactile-dependent plasticity. These results show that AFD uses distinct sets of guanylyl cyclases to execute dual roles: precise temperature sensing and tactile-dependent behavioral modulation.

Differential regulation of context-dependent plasticity and basal locomotion rates in AFD

Our results further suggest that the mechanisms controlling basal locomotion and context-dependent behavioral modulation are not only distinct but also operate independently. Temperature fluctuations significantly affect basal locomotion rates, i.e., higher temperatures accelerate speed, while lower temperatures slow it down [67,68]. However, tactile-dependent

locomotion modulation in microfluidic chambers remains robust despite these temperature-induced changes in basal movement. This independence is further supported by our observations in *tax-4* and *kcc-3* mutants, which display elevated basal locomotion rates yet still adjust their locomotion in response to tactile experiences. These findings indicate that the processes governing basal locomotion and context-dependent modulation are controlled by separate, non-interfering mechanisms, even though both pathways engage cGMP signaling.

Electrical synapses link the thermosensory neuron AFD to tactile-dependent behavioral modulation

AIB-AFD electrical synapses are pivotal for tactile-dependent behavioral plasticity. Disrupting this connection impairs tactile-dependent locomotion modulation, whereas restoring an engineered electrical synapse rescues this behavior. The successful replacement of invertebrate innexins with vertebrate connexins, which perform analogous functions despite lacking sequence homology, indicates that the core function of these synapses lies in their connectivity rather than in their specific protein sequences. This observation suggests that the transfer of signaling molecules such as Ca^{2+} and cGMP through electrical synapses may facilitate the coordination of neuronal activity across distinct networks [103–106].

Together, these findings support a model in which AIB functions as a hub neuron that relays mechanosensory input from FLP to AFD to modulate locomotion (Fig. 5C). However, because electrical synapses are often bidirectional, information flow may also occur in the opposite direction, from AFD to AIB. Determining the directionality and dynamics of this signaling remains an important question for future investigation. A similar circuit logic has been proposed for thermal avoidance behavior, in which AIB integrates inputs from FLP via chemical synapses and couples to AFD via electrical synapses, forming an FLP-AIB-AFD circuit. In that case, the directionality of information flow also remains unresolved [107].

Finally, the proposed circuit mechanism for tactile-dependent modulation does not exclude additional routes of modulation. These may include extra-synaptic signaling mechanisms, such as neuropeptide release from other touch-sensitive neurons. While the precise molecular and circuit mechanisms remain to be elucidated, our findings establish that AIB-AFD electrical synapses are essential for incorporating tactile context into locomotor control.

In summary, our findings reveal an unexpected role for AFD in tactile-dependent behavioral plasticity. They show that specialized molecular mechanisms, including distinct cGMP signaling pathways, diverse guanylyl cyclases, and functional electrical synapse connectivity, enable AFD sensory neurons to perform dual functions: detect stimuli and support tactile-dependent plasticity. A limitation of this study is that the directionality and mode of information flow between AFD and AIB remain unresolved, and defining this relationship will be an important goal for future investigation. Nevertheless, our results establish the AFD-AIB connection as a regulatory hub in tactile-dependent locomotor modulation and expand our understanding of sensory neuron versatility in adaptive behavior.

Methods

Nematode Strains and Growth

C. elegans strains were maintained under standard conditions at 20°C on nematode growth medium (NGM) agar plates [108]. These plates were seeded with *E. coli* OP50 lawns. Strains used in this study are listed in Table S1 and are available from the corresponding author upon request.

Molecular Biology

All DNA constructs were sequence-verified. cDNA sequences encoding *mec-10*, *cng-3*, and *inx-10* were amplified from a cDNA library made with the SuperScript III Reverse Transcriptase kit (Thermo Fisher Scientific, MA) from total RNA extracted from adult N2 worms. A codon-optimized cDNA sequence for the mouse gap junction protein connexin-36 (Cx36) was previously described

[109]. DNA plasmid constructs for *C. elegans* expression were assembled by LR recombination using the MultiSite Gateway Three-Fragment Vector Construction Kit (Thermo Fisher Scientific, MA). Entry clones were constructed as follows: (i) promoter sequences flanked by attL4 and attR1 sites; (ii) cDNA sequences flanked by attL1 and attL2 sites; and (iii) *sl2::mNeonGreen::rab-3 3'utr* flanked by attR2 and attL3 sites. Destination vectors used for LR recombination included the pDEST R4-R3 Vector II and a custom-built destination vector BJP-C957, which contains a hygromycin resistance cassette for selection, an intestinal fluorescent marker (*vha-6p::mScarlet::tbb-2 3'utr*) for visual screening transgenic worms, and flanking *mos1* sequences to facilitate homologous recombination for Mos1-mediated single-copy insertion (MosSCI). Promoters used for tissue- or cell-specific expression were: *gcy-18p* (2 kb) and *srtx-1Bp* (493 bp) for AFD; *mec-18p* (390 bp) for TRNs; *egl-44p* (5 kb) for FLP; *inx-1p* (1kb) for AIB, and *mec-10p* (3 kb) for expression in TRNs, FLP, and PVD. Plasmids used to generate transgenic strains in this study are listed in Table S2.

Transgenes, Germline Transformation, and Genome Editing

Strains carrying extrachromosomal arrays were generated by microinjecting various plasmids together with co-injection markers. The co-injection markers included *unc-112p::gfp* (30 ng/µl), *rpl-28p::neoR* (20 ng/µl), and *Cbr-unc-119* (20 ng/µl). The blank vector pBluescript was used as filler DNA to bring the final total DNA concentration to 100 ng/µl. A detailed list of the plasmids used to create transgenic worms in this study is provided in Table S2.

Mos1-mediated transgene insertion [110,111] was used to generate single-copy transgenic animals. Briefly, worms carrying the *ttTi5605 Mos1* site on chromosome II were injected with a plasmid mixture containing the transgene of interest (40 ng/µl), along with BJP-B908, a plasmid expressing Cas9 and a guide RNA targeting the Mos1 site (60 ng/µl). Selection markers included *rps-0p::hygR* for hygromycin resistance and *vha-9p::mScarlet* for intestinal red fluorescence to enable visual screening.

The *gcy-18::gfp11×7* knock-in strain was generated using a modified CRISPR–Cas9 protocol employing preassembled Cas9 ribonucleoprotein (RNP) complexes, co-injected with a single-stranded DNA repair template to facilitate homologous recombination [112,113]. Cas9 protein and crRNA (targeting sequence: TACAACGACTGAAAGAGGAG) were obtained from Integrated DNA Technologies (IDT, NJ). The single-stranded DNA repair template for generating *gcy-18::gfp11×7* was synthesized by Twist Bioscience. Successful editing produced the *pek331* allele, which carries an in-frame GFP11×7 insertion at the C-terminus of GCY-18. The insertion was verified by PCR and DNA sequencing. A worm strain, BJH833, carrying both *pek331* and *muIs253 [eft-3p::sfgfp1-10::unc-54 3'utr]*, was used to visualize GCY-18 by complemented split-GFP fluorescence [114].

Fabrication of PDMS Microfluidic Chambers

Microfluidic chamber designs were created in AutoCAD and fabricated as 100 µm SU8-silicon molds using photolithography (FlowJem, NO, Canada). PDMS devices were produced by pouring degassed PDMS prepolymer (Sylgard 184, Dow Corning, MI) onto the molds, degassing again under vacuum (−25 inHg, 15 min, room temperature), and curing at 80 °C for 2 hours. The cured PDMS was peeled from the mold, and inlet/outlet ports were punched using a 2 mm biopsy punch (Acuderm Inc., FL). For the chambers with a removable barrier shown in Figure 1–Supplement 1A, cast PDMS chamber structures were bonded onto a thin semi-cured PDMS sheet to create a permanent, watertight seal. To prepare the sheet, ~30 ml of PDMS was poured into a 6-inch Petri dish, degassed for 15 min, and partially cured at 65 °C for 15-20 min, until firm but still tacky. PDMS chamber structures were gently placed onto the sheet with ~2 mm spacing to allow the formation of a barrier, then fully cured at 80 °C for 30 min. PDMS devices were bonded to 1 mm glass microscope slides using oxygen plasma treatment (PDC-32G, Harrick Scientific, NY, 1 min).

Behavior Recording and Analysis

Videos were captured for 10 seconds at 7.5 frames per second using a Basler acA2440 camera (Basler, PA) equipped with an AF Micro-NIKKOR 60 mm lens (Nikon, NY). Behavioral data were extracted from the videos using WormLab software (MBF Bioscience, VT) through individual worm tracking. Only those worms that were already within the assay area at the start of the recording were analyzed, and any worms that entered later were excluded. Crawling speed was determined by the total distance traveled by a worm during the 10 second recordings. A turn was defined as a change in crawling direction of 15° or more. Reversals were defined as sudden movement in the opposite direction for at least 5 frames (~0.6 seconds). Worms were considered idle if their absolute velocity (distance traveled between frames) was below 20 μm/s for more than 10 frames (~1.3 seconds).

For behavior analysis, worms were age-synchronized by transferring 30-50 young adult worms onto an NGM plate seeded with OP50 and allowing them to lay eggs for 2 hours before removal. The plates were then kept at room temperature (22°C) for 3 days, allowing the eggs to develop into young adults, identified by the presence of 5-10 eggs arranged in single rows within the gonads of all worms on the plate. To wash the synchronized adults off the plate, worms were gently transferred into Eppendorf tubes using glass Pasteur pipettes. After allowing the worms to settle at the bottom of the tube (~1 minute), the supernatant was removed and replaced with fresh M9 buffer. This washing step was repeated three times to remove residual OP50. Next, approximately 30-70 worms were loaded into an inlet of the chambers shown in Figure 1 using a 20μl pipette and allowed to roam freely in the chamber for 60 minutes before behavior in the assay area was recorded.

To assay worms confined to the assay area by a barrier (Fig. 1–Supplement 1A), PDMS chambers were prepared with a removable gap separating the training and assay zones. M9 buffer was first injected into the exploration zone, after which ~100 worms were loaded and allowed to explore for 10 minutes, during which they moved only within the reach of the M9 buffer, typically up to the gap between the exploration and assay zones. To remove the barrier, additional M9 buffer was gently introduced into the assay zone until it merged with the buffer, allowing worms to move freely between zones. After 15 minutes of exploration, the barrier was reintroduced by completely drying the space between the zones with a Kimwipe, once again confining worms to areas containing M9 buffer. Behavior in the assay zone was recorded immediately after the barrier was reinserted and again 40 minutes later.

Fluorescence microscopy

Widefield fluorescence microscopy was performed using a Leica DMi8 inverted microscope equipped with 63x/1.4NA and 100x/1.4NA oil-immersion objectives (Leica Biosystems, NJ). Worms were mounted on thin 3% agar pads and anesthetized with 10 mM levamisole diluted in M9 buffer. Images were acquired with an Andor iXon-888 EMCCD camera (Oxford Instruments, England), with an exposure time of 150 ms and an electron-multiplying (EM) gain of 200. Acquisition settings were kept constant across experiments.

Statistical Analysis

Behavior measurements were calculated for each individual chamber, and these chamber-specific values were then used to generate the final mean values shown in the bar plots. The sample size was defined as the number (approximately 25) of chambers analyzed per experiment. An unpaired Student's t-test with Bonferroni correction was used to compare average speeds between uniform and binary chambers. To quantify the relative difference between groups, we calculated the percent change for each value in the uniform chambers relative to the mean of value from the binary chambers. Specifically, we subtracted the mean of the values from the binary chamber from each individual value in the uniform chamber. The result was then divided by the mean of

the binary chamber and multiplied by 100 to express the difference as a percentage. For comparisons among multiple strains, we conducted one-way ANOVA followed by a Tukey–Kramer post hoc test on all possible pairwise comparisons. All statistical analyses were performed using R.

Figure supplements

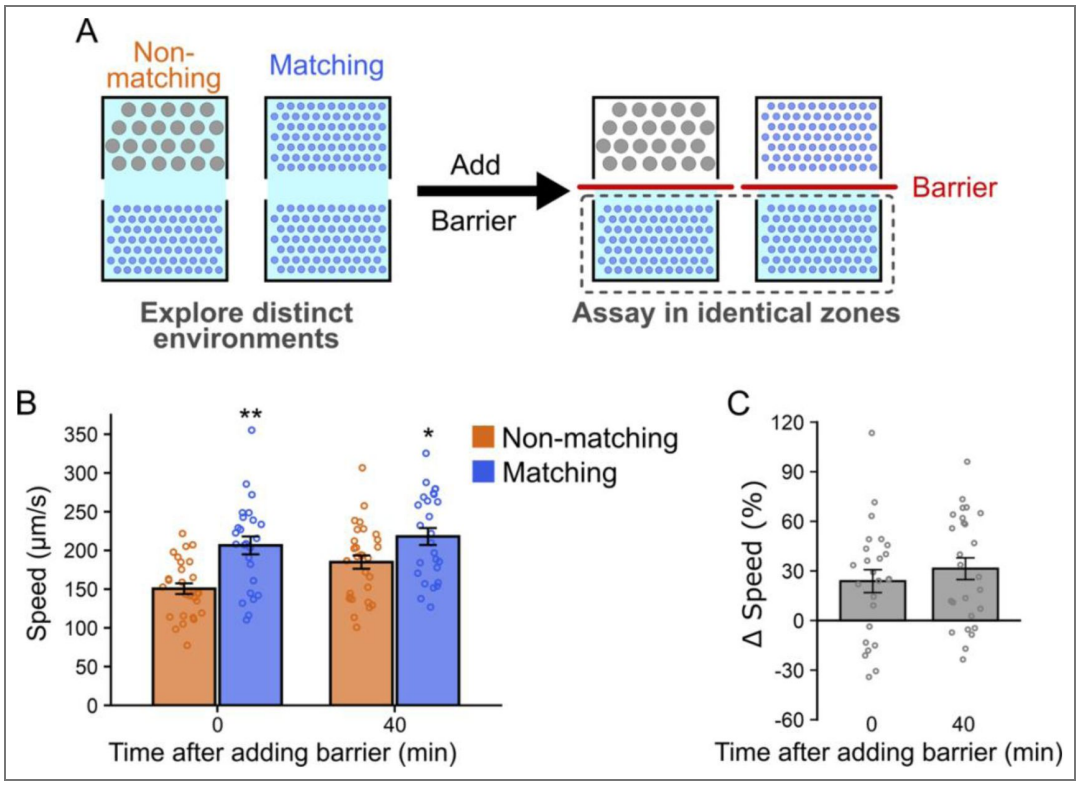

Figure 1–Supplement 1. Prior exploration of distinct physical settings modulates locomotion speed of worms in identical environments. (A) Schematic of the chamber design with separate exploration and assay zones divided by a removable barrier. The assay zone was identical across conditions, whereas the exploration zone contained physical settings that were either matching or non-matching relative to the assay zone. Worms explored these settings before entering the assay zone, where they were confined by insertion of a barrier. (B) Quantification of locomotion speed for wild type N2 worms in the assay area was performed either immediately after inserting the barrier or 40 minutes later (matching: n = 25; non-matching: n = 28). Asterisks indicate statistically significant difference between matching and non-matching chambers (unpaired Student's *t*-test; *: p <0.05; **: p < 0.01). (C) The percent change in locomotion speed (Δspeed) between worms that had explored matching and non-matching chambers was calculated and normalized to the mean value of the non-matching condition. Data are presented as mean ± SEM, with each point representing the mean value of worms within a single chamber.

Figure 2–Supplement 1. Guanylyl cyclase genes *gcy-18* and *gcy-12* are required for spatial preference, but only *gcy-18* supports context-dependent locomotion modulation.

(A) A small-scale screen of guanylyl cyclase genes required for spatial preference in microfluidic chambers. Preference index values were calculated as previously described [52]. Wild type worms exhibited a strong preference for area IV, the preferred region of the chamber [52], whereas *gcy-18(gk423024)* and *gcy-12(gk142661)* mutants showed significantly reduced preference. Data are shown as mean ± SEM; each point represents the mean value from one chamber. Statistical comparisons were performed using Dunnett's test for multiple comparisons (** $p < 0.01$). (B) Speed differences (Δspeed) between uniform and binary chambers in wild type N2 and *gcy-12* mutant worms. *gcy-12* mutants displayed context-dependent locomotion modulation comparable to wild type. Data are shown as mean ± SEM; each point represents the mean behavior of worms within a single chamber. Statistical significance was determined using an unpaired Student's t-test (n.s., $p > 0.05$).

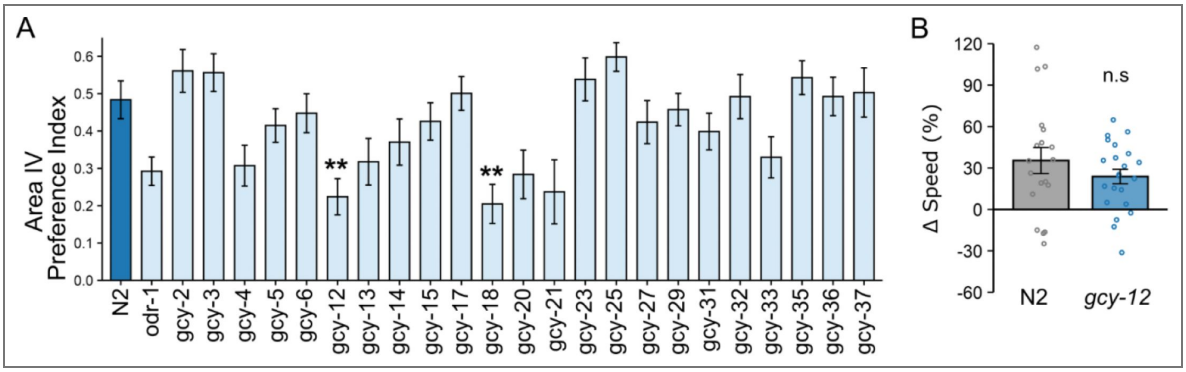

Figure 3–Supplement 1. Temperature shifts alter absolute locomotion speed but do not affect context-dependent locomotion modulation.

(A) Experimental design. Worms were cultivated at 17°C, 20°C, or 23°C and then transferred to 20°C for 1 hour before behavioral recording. (B) Locomotion speed of wild type N2 worms in the binary (left) and uniform (right) chambers after experiencing temperature shifts (+3°C: uniform n = 32; binary n = 31; 0°C: uniform n = 30; binary n = 29; -3°C: uniform n = 36; binary n = 35). Linear regression identified a significant positive correlation between rearing temperature and locomotion speed in both chambers. (C) Differences in speed (Δspeed) across temperature-shift conditions. Linear regression analysis revealed no significant relationship between Δspeed and temperature shift. Data are shown as mean ± SEM.

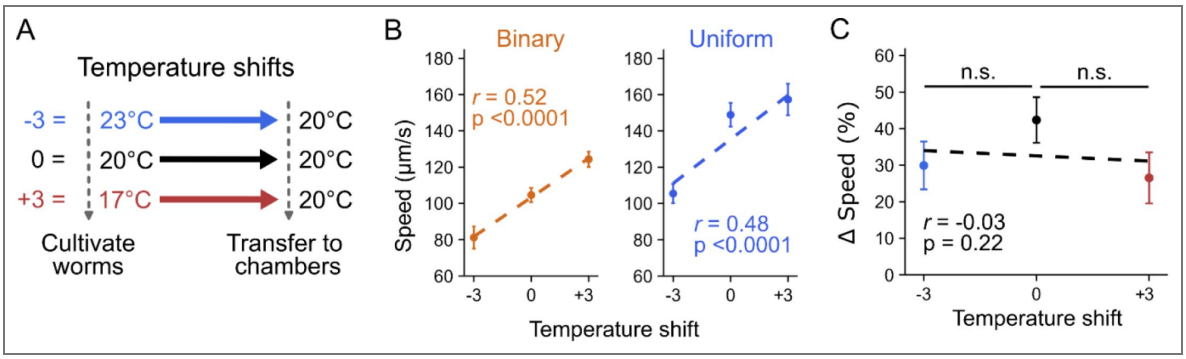

Fig. 4–Supplement 1. GCY-18 primarily localizes to AFD dendritic endings and remains detectable in *kcc-3* and *ttx-1* mutants.

GCY-18 was visualized using a split-GFP strategy (GCY-18::GFP11x7 complemented by GFP1-10). (A-C) Representative images of the head region of wild type (A), *kcc-3* mutant (B), and *ttx-1* mutant (C) worms. Left panels show brightfield images overlaid with GFP fluorescence. Middle panels (A'-C') show GFP fluorescence alone. Right panels show higher-magnification views of the distal dendritic ending (nose region; A''-C'') and regions near the AFD soma and axon (A'''-C'''). Dashed boxes in the middle panels indicate the approximate regions shown at higher magnification in the right panels.

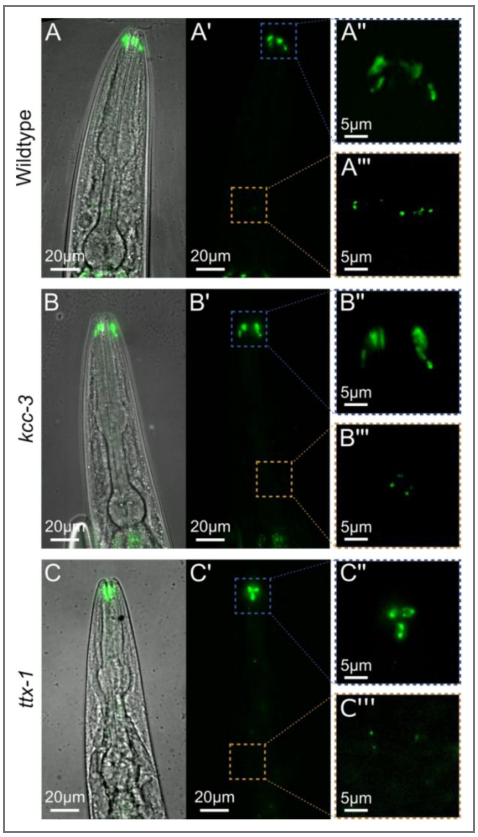

Figure 4–Supplement 2.

(A) AFD-ablated and *gcy-18* mutant worms that experienced different exploration zones show impaired locomotion speed adjustment when confined to the assay zone by a removable barrier. Δspeed values for wild type N2 (matching: n = 25; non-matching: n = 28), *gcy-18* mutants (matching: n = 22; non-matching: n = 17), and AFD-ablated worms (matching: n = 26; non-matching: n = 26). Data are presented as mean ± SEM, with each point representing the mean locomotion speed value of worms within a single chamber. (B) Locomotion rates of wild type (n = 15), *gcy-18* mutants (n = 10), and AFD-ablated worms (n = 18) are comparable on NGM plates. (C) Body lengths of wild type, *gcy-18* mutant, and AFD-ablated worms are not significantly different. Data are shown as Mean ± SEM, with each point representing an individual animal (Dunnett's test, *p < 0.05; n.s., p > 0.05).

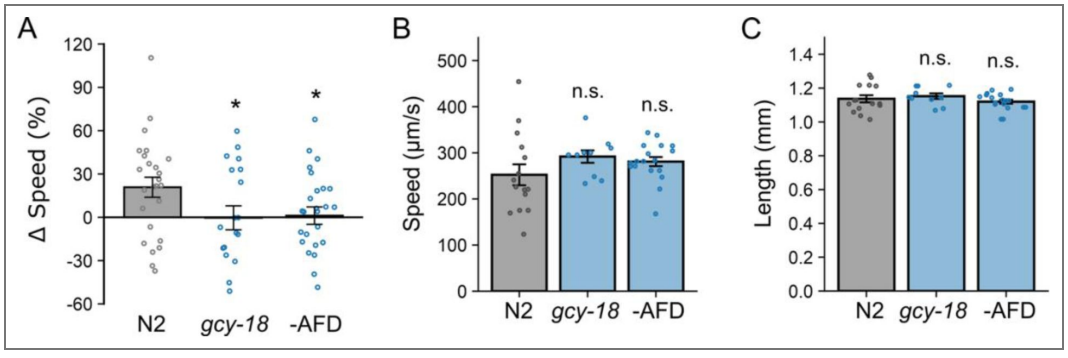

Strain	Genotype	Source
CX2065	*odr-1(n1936) X*	CGC
VC3024	*gcy-2(ok3721) II*	CGC
VC2796	*gcy-3(gk1154) II*	CGC
VC20038	*gcy-4(gk152604) II*	CGC
VC20321	*gcy-6(gk245152) V*	CGC
RB1000	*gcy-5(ok921) II*	CGC
VC20321	*gcy-6(gk245152) V*	CGC
VC20451	*gcy-12(gk142661) II*	CGC
VC3242	*gcy-13(gk3189) V*	CGC
JN1194	*gcy-14(pe1102) V*	CGC
VC2675	*gcy-15(gk1102) II*	CGC
VC2450	*gcy-17(gk1155) I*	CGC
VC30137	*gcy-18(gk423024) IV*	CGC
RB1935	*gcy-20(ok2538) V*	CGC
VC40920	*gcy-21(gk882422) II*	CGC
RB924	*gcy-23(ok797) IV*	CGC
VC2375	*gcy-25(gk1187) IV*	CGC
RB2622	*gcy-27(ok3653) IV*	CGC
VC20193	*gcy-29(gk162111) II*	CGC
CZ3714	*gcy-31(ok296) X*	CGC
RB1048	*gcy-32(ok995) V*	CGC
CZ3715	*gcy-33(ok232) V*	CGC
CX6448	*gcy-35(ok769) I*	CGC
AX1297	*gcy-36(db66) X*	CGC
RB626	*gcy-37(ok384) IV*	CGC
PR694	*tax-2(p694) I*	CGC
PR678	*tax-4(p678) III*	CGC
FX31482	*cng-2(tm4267) IV*	NBRP, Japan
VC40261	*cng-3(gk541751) IV*	CGC
VC20290	*cng-4(gk195496) IV*	CGC
IK800	*gcy-8(oy44) IV*	CGC
IK429	*gcy-18(nj38) IV*	CGC
VC20451	*gcy-12(gk142661) II*	CGC
BJH2598	*cng-3(gk541751) IV; ttTi5605 II*	This study
BJH2596	*gcy-18(gk423024)* IV*; ttTi5605* II	This study
BJH3481	*pekSi609[gcy-18p::gcy-18::sl2::mNeonGreen::rab-3 3'utr; vha-6p::mScarlet; hygR(+)] ttTi5605 II; gcy-18(gk423024) IV*	This study
BJH3527	*pekSi655[srtx-1Bp::cng-3::sl2::mNeonGreen::rab-3 3'utr; vha-6p::mScarlet; hygR(+)] ttTi5605 II; cng-3(gk541751) IV*	This study

Table S1. **Strains used in this study**

BJH3539	*pekSi667[gcy-18p::cng-3::sl2::mNeonGreen::unc-54 3'utr; vha-6p::mScarlet; hygR(+)] ttTi5605 II; cng-3(gk541751) IV*	This study
GN112	*pgIs2[gcy-8p::TU#813; gcy-8p::TU#814; unc-122p::gfp; gcy-8p::mCherry; gcy-8p::gfp; ttx-3p::gfp]*	CGC
LX1024	*kcc-3(ok228) II*	Gift from the Singhvi Lab
PR767	*ttx-1(p767) V*	CGC
JN578	*peIs578 [npr-9p::casp1; npr-9p::Venus; unc-122p::mCherry]*	CGC
ZB2551	*mec-10 (tm1552) X*	CGC
BJH976	*pekSi102[egl-44p::mec-10::unc-54 3'utr; neoR(+)] ttTi5605 II; mec-10(tm1552) X.*	This study
BJH977	*pekSi103[mec-18p::mec-10::unc-54 3'utr; neoR(+)] ttTi5605 II; mec-10(tm1552) X.*	This study
BJH978	*pekSi104[mec-10p::mec-10::unc-54 3'utr; neoR(+)] ttTi5605 II; mec-10(tm1552) X.*	This study
BJH4059	*pekSi102[egl-44p::mec-10::unc-54 3'utr; neoR(+)] ttTi5605 II; pekSi715[mec-18p::mec-10::unc-54 3'utr; neoR(+)] cxTi10816 IV; mec-10(tm1552) X*	This study
FG927	*inx-1(tm6662)* X.	CGC
FG0614	*inx-4 (ok2373) V*	Gift from the Ferkey lab
RB1792	*inx-7(ok2319)* IV	CGC
RB2051	*inx-10(ok2714) V*	CGC
FX01896	*inx-19 (tm1896) I*	NBRP, Japan
BJH2919	*inx-7(ok2319) IV; inx-10(ok2714) V*	This study
BJH1162	*pekEx302 [srtx-1Bp::cx36::sl2::mNeonGreen; inx-1p::cx36::sl2::mKate; Cbr-unc-119(+); unc-122p::gfp; neoR(+)]; unc-119(ed3) III; inx-7(ok2319) IV; inx-10(ok2714) V*	This study
BJH4060	*pekSi717[srtx-1Bp::inx-10a(genomic)::sl2::gfp::let-858 3' UTR; vha-6p::mScarlet; HygR(+)] ttTi5605 II; inx-10(ok2714) V*	This study
BJH833	*muIs253[eft-3p::gfp1-10::unc-54 3'utr; Cbr-unc-119(+)]; unc-119(ed3) III; gcy-18(pek331[gcy-18::gfp11x7]) IV*	This study
BJH4056	*muIs253[eft-3p::gfp1-10::unc-54 3'utr, Cbr-unc-119(+)]; kcc-3(ok228) II; gcy-18(pek331[gcy-18::gfp11x7]) IV*	This study
BJH4057	*muIs253[eft-3p::gfp1-10::unc-54 3'utr, Cbr-unc-119(+)]; gcy-18(pek331[gcy-18::gfp11x7]) IV; ttx-1(p767) V*	This study

CGC: Caenorhabditis Genetics Center.

NBRP: National BioResource Project.

Table S1. (continued)

Name	Constructs
BJP-MR16	*gcy-18p::gcy-18::sl2::mNeonGreen::rab-3 3'utr; vha-6p::mScarlet::tbb-2 3'utr; hygR(+)*
BJP-MR65	*srtx-1Bp::cng-3::sl2::mNeonGreen::rab-3 3'utr; vha-6p::mScarlet::tbb-2 3'utr; hygR(+)*
BJP-MR93	*gcy-18p::cng-3::sl2::mNeonGreen::rab-3 3'utr; vha-6p::mScarlet::tbb-2 3'utr; hygR(+)*
BJP-MR96	*inx-1p::cx36::sl2::mKate::rab-3 3'utr*
BJP-MR97	*srtx-1bp::cx36::sl2::mKate::rab-3 3'utr*
BJP-A433	*mec-18p::mec-10::unc-54 3'utr; neoR(+)*
BJP-A433	*egl-44p::mec-10::unc-54 3'utr; neoR(+)*

Table S2. Plasmids used to generate transgenic strains in this study

Data availability

The data supporting the findings of this study are available in Dryad at *https://doi.org/10.5061/dryad.k3j9kd5pz*.

Acknowledgements

This research was supported by NIH grants R01NS109476 and R01NS115974 to JB. MR was supported by T32GM136534 and F31NS129545. The authors thank the Caenorhabditis elegans Genetics Center (funded by the NIH Office of Research Infrastructure Programs P40 OD010440) for providing worm strains. We also thank Lin Zhang and Yan Liu for their support in constructing DNA plasmids and generating transgenic worm strains. Special thanks to Melissa Woo (Mercer Island High School), Tabitha Ngo, and Sahithi Challam (Interlake High School) for their assistance with worm maintenance. We appreciate the members of the Bai lab for their critical reading of the manuscript. Additionally, we acknowledge the multiple mentorship programs at Fred Hutchinson Cancer Center, including the SURP Undergraduate Researchers and Pathways Undergraduate Researchers programs, supported in part by the Cancer Center Support Grant P30 CA015704, for fostering relationships with high school and undergraduate trainees who contributed to this project.

Additional information

Funding

Funder	Grant reference number	Author
HHS | NIH | National Institute of Neurological Disorders and Stroke (NINDS)	R01NS109476	Jihong Bai
HHS | NIH | National Institute of Neurological Disorders and Stroke (NINDS)	R01NS115974	Jihong Bai
HHS | NIH | National Institute of General Medical Sciences (NIGMS)	T32GM136534	Manuel Rosero
HHS | NIH | National Institute of Neurological Disorders and Stroke (NINDS)	F31NS129545	Manuel Rosero
HHS | NIH | National Cancer Institute (NCI)	P30CA015704	Jihong Bai

Author ORCID iDs

Manuel Rosero: https://orcid.org/0000-0001-8950-7251
Jihong Bai: https://orcid.org/0000-0001-6773-2175

References

1. **Navarro-Sánchez M,** Gil-Miravet I, Montero-Caballero D, Castillo-Gómez E, Gundlach AL, Olucha-Bordonau FE (2024) Some key parameters in contextual fear conditioning and extinction in adult rats. *Behavioural Brain Research* **462**:114874 https://doi.org/10.1016/j.bbr.2024.114874
2. **Maren S,** Phan KL, Liberzon I (2013) The contextual brain: implications for fear conditioning, extinction and psychopathology. *Nat Rev Neurosci* **14**:417-428 https://doi.org/10.1038/nrn3492
3. **Battaglia S** (2018) Garofalo S, di Pellegrino G. Context-dependent extinction of threat memories: influences of healthy aging. *Scientific Reports* **8** https://doi.org/10.1038/s41598-018-31000-9
4. **Leitman DI,** Wolf DH, Loughead J, Valdez JN, Kohler CG, Brensinger C, et al. (2011) Ventrolateral prefrontal cortex and the effects of task demand context on facial affect appraisal in schizophrenia. *Soc Cogn Affect Neurosci* **6**:66-73 https://doi.org/10.1093/scan/nsq018

5. **Hadjikhani N,** Joseph RM, Manoach DS, Naik P, Snyder J, Dominick K, et al. (2009) Body expressions of emotion do not trigger fear contagion in autism spectrum disorder. *Social Cognitive and Affective Neuroscience* **4**:70-78 https://doi.org/10.1093/scan/nsn038

6. **Kipps CM,** Nestor PJ, Acosta-Cabronero J, Arnold R, Hodges JR (2009) Understanding social dysfunction in the behavioural variant of frontotemporal dementia: the role of emotion and sarcasm processing. *Brain* **132**:592-603 https://doi.org/10.1093/brain/awn314

7. **Greimel E,** Nehrkorn B, Fink GR, Kukolja J, Kohls G, Müller K, et al. (2012) Neural mechanisms of encoding social and non-social context information in autism spectrum disorder. *Neuropsychologia* **50**:3440-3449 https://doi.org/10.1016/j.neuropsychologia.2012.09.029

8. **Badel L,** Ohta K, Tsuchimoto Y, Kazama H (2016) Decoding of Context-Dependent Olfactory Behavior in Drosophila. *Neuron* **91**:155-167 https://doi.org/10.1016/j.neuron.2016.05.022

9. **Haberkern H,** Basnak MA, Ahanonu B, Schauder D, Cohen JD, Bolstad M, et al. (2019) Visually Guided Behavior and Optogenetically Induced Learning in Head-Fixed Flies Exploring a Virtual Landscape. *Current Biology* **29**:1647-1659.e8. https://doi.org/10.1016/j.cub.2019.04.033

10. **Sheintuch L,** Geva N, Baumer H, Rechavi Y, Rubin A, Ziv Y (2020) Multiple Maps of the Same Spatial Context Can Stably Coexist in the Mouse Hippocampus. *Current Biology* **30**:1467-1476.e6. https://doi.org/10.1016/j.cub.2020.02.018

11. **Zars M,** Zars T (2006) High and low temperatures have unequal reinforcing properties in Drosophila spatial learning. *J Comp Physiol A* **192**:727-735 https://doi.org/10.1007/s00359-006-0109-6

12. **Kishimoto Y,** Kasamatsu S, Yanai S, Endo S, Akaike T, Ihara H (2019) 8-Nitro-cGMP attenuates context-dependent fear memory in mice. *Biochemical and Biophysical Research Communications* **511**:141-147 https://doi.org/10.1016/j.bbrc.2019.01.138

13. **Sasaki A,** Sotnikova TD, Gainetdinov RR, Jarvis ED (2006) Social Context-Dependent Singing-Regulated Dopamine. *J Neurosci* **26**:9010-9014 https://doi.org/10.1523/JNEUROSCI.1335-06.2006

14. **Billeter J-C,** Jagadeesh S, Stepek N, Azanchi R, Levine JD (2012) Drosophila melanogaster females change mating behaviour and offspring production based on social context. *Proceedings of the Royal Society B: Biological Sciences* **279**:2417-2425 https://doi.org/10.1098/rspb.2011.2676

15. **Wolfin MS,** Raguso RA, Davidowitz G, Goyret J (2018) Context dependency of in-flight responses by Manduca sexta moths to ambient differences in relative humidity. *Journal of Experimental Biology* **221** https://doi.org/10.1242/jeb.177774

16. **Sawin ER,** Ranganathan R, Horvitz HR (2000) C. elegans Locomotory Rate Is Modulated by the Environment through a Dopaminergic Pathway and by Experience through a Serotonergic Pathway. *Neuron* **26**:619-631 https://doi.org/10.1016/S0896-6273(00)81199-X

17. **Gourgou E,** Adiga K, Goettemoeller A, Chen C, Hsu A-L (2021) *Caenorhabditis elegans* learning in a structured maze is a multisensory behavior. *iScience* **24** https://doi.org/10.1016/j.isci.2021.102284

18. **Dillon J,** Holden-Dye L, O'Connor V, Hopper NA (2016) Context-dependent regulation of feeding behaviour by the insulin receptor, DAF-2, in Caenorhabditis elegans. *Invert Neurosci.* **16**:: 4 https://doi.org/10.1007/s10158-016-0187-2

19. **Law E,** Nuttley WM, Kooy D van der (2004) Contextual Taste Cues Modulate Olfactory Learning in C. elegans by an Occasion-Setting Mechanism. *Current Biology* **14**:1303-1308 https://doi.org/10.1016/j.cub.2004.06.066

20. **Kindt KS,** Quast KB, Giles AC, De S, Hendrey D, Nicastro I, et al. (2007) Dopamine Mediates Context-Dependent Modulation of Sensory Plasticity in C. elegans. *Neuron* **55**:662-676 https://doi.org/10.1016/j.neuron.2007.07.023

21. **Goetting DL,** Soto R, Van Buskirk C (2018) Food-Dependent Plasticity in Caenorhabditis elegans Stress-Induced Sleep Is Mediated by TOR-FOXA and TGF-β Signaling. *Genetics* **209**:1183-1195 https://doi.org/10.1534/genetics.118.301204

22. **Susoy V,** Hung W, Witvliet D, Whitener JE, Wu M, Park CF, et al. (2021) Natural sensory context drives diverse brain-wide activity during C. elegans mating. *Cell* https://doi.org/10.1016/j.cell.2021.08.024

23. **Ghosh DD,** Sanders T, Hong S, McCurdy LY, Chase DL, Cohen N, et al. (2016) Neural Architecture of Hunger-Dependent Multisensory Decision Making in *C. elegans*. *Neuron* **92**:1049-1062 https://doi.org/10.1016/j.neuron.2016.10.030
24. **Zhen M,** Samuel AD (2015) C. elegans locomotion: small circuits, complex functions. *Current Opinion in Neurobiology* **33**:117-126 https://doi.org/10.1016/j.conb.2015.03.009
25. **Emmons SW** (2018) Neural Circuits of Sexual Behavior in Caenorhabditis elegans. *Annual Review of Neuroscience* **41**:349-369 https://doi.org/10.1146/annurev-neuro-070815-014056
26. **Meisel JD,** Kim DH (2014) Behavioral avoidance of pathogenic bacteria by Caenorhabditis elegans. *Trends in Immunology* **35**:465-470 https://doi.org/10.1016/j.it.2014.08.008
27. **Metaxakis A,** Petratou D, Tavernarakis N (2018) Multimodal sensory processing in Caenorhabditis elegans. *Open Biol* **8** https://doi.org/10.1098/rsob.180049
28. **Stout RF,** Verkhratsky A, Parpura V (2014) Caenorhabditis elegans glia modulate neuronal activity and behavior. *Front Cell Neurosci* **8** https://doi.org/10.3389/fncel.2014.00067
29. **Ward S,** Thomson N, White JG, Brenner S (1975) Electron microscopical reconstruction of the anterior sensory anatomy of the nematode caenorhabditis elegans. *Journal of Comparative Neurology* **160**:313-337 https://doi.org/10.1002/cne.901600305
30. **Ware RW,** Clark D, Crossland K, Russell RL (1975) The nerve ring of the nematode Caenorhabditis elegans: Sensory input and motor output. *Journal of Comparative Neurology* **162**:71-110 https://doi.org/10.1002/cne.901620106
31. **Ghosh DD,** Nitabach MN, Zhang Y, Harris G (2017) Multisensory integration in C. elegans. *Current Opinion in Neurobiology* **43**:110-118 https://doi.org/10.1016/j.conb.2017.01.005
32. **Hobert O** (2003) Behavioral plasticity in C. elegans: Paradigms, circuits, genes. *Journal of Neurobiology* **54**:203-223 https://doi.org/10.1002/neu.10168
33. **Komuniecki R,** Hapiak V, Harris G, Bamber B (2014) Context-dependent modulation reconfigures interactive sensory-mediated microcircuits in Caenorhabditis elegans. *Current Opinion in Neurobiology* **29**:17-24 https://doi.org/10.1016/j.conb.2014.04.006
34. **Goodman MB,** Sengupta P (2018) The extraordinary AFD thermosensor of C. elegans. *Pflugers Arch - Eur J Physiol* **470**:839-849 https://doi.org/10.1007/s00424-017-2089-5
35. **Clark DA,** Biron D, Sengupta P, Samuel ADT (2006) The AFD Sensory Neurons Encode Multiple Functions Underlying Thermotactic Behavior in Caenorhabditis elegans. *J Neurosci* **26**:7444-7451 https://doi.org/10.1523/JNEUROSCI.1137-06.2006
36. **Yoshida A,** Nakano S, Suzuki T, Ihara K, Higashiyama T, Mori I (2016) A glial K+/Cl− cotransporter modifies temperature-evoked dynamics in Caenorhabditis elegans sensory neurons. Genes. *Brain and Behavior* **15**:429-440 https://doi.org/10.1111/gbb.12260
37. **Singhvi A,** Liu B, Friedman CJ, Fong J, Lu Y, Huang X-Y, et al. (2016) A Glial K/Cl Transporter Controls Neuronal Receptive Ending Shape by Chloride Inhibition of an rGC. *Cell* **165**:936-948 https://doi.org/10.1016/j.cell.2016.03.026
38. **Satterlee JS,** Sasakura H, Kuhara A, Berkeley M, Mori I, Sengupta P (2001) Specification of Thermosensory Neuron Fate in C. elegans Requires ttx-1, a Homolog of otd/Otx. *Neuron* **31**:943-956 https://doi.org/10.1016/S0896-6273(01)00431-7
39. **Aok I,** Shiota M, Tsukada Y, Nakano S, Mori I (2022) cGMP dynamics that underlies thermosensation in temperature-sensing neuron regulates thermotaxis behavior in C. elegans. *PLOS One* **17**:e0278343 https://doi.org/10.1371/journal.pone.0278343
40. **Ramot D,** MacInnis BL, Goodman MB (2008) Bidirectional temperature-sensing by a single thermosensory neuron in C. elegans. *Nat Neurosci* **11**:908-915 https://doi.org/10.1038/nn.2157
41. **Wang D,** O'Halloran D, Goodman MB (2013) GCY-8, PDE-2, and NCS-1 are critical elements of the cGMP-dependent thermotransduction cascade in the AFD neurons responsible for C. elegans thermotaxis. . *J Gen Physiol* **142**:: 437-449 https://doi.org/10.1085/jgp.201310959

42. **Takeishi A,** Yu YV, Hapiak VM, Bell HW, O'Leary T, Sengupta P (2016) Receptor-type Guanylyl Cyclases Confer Thermosensory Responses in C. elegans. *Neuron* **90**:235-244 https://doi.org/10.1016/j.neuron.2016.03.002

43. **Inada H,** Ito H, Satterlee J, Sengupta P, Matsumoto K, Mori I (2006) Identification of Guanylyl Cyclases That Function in Thermosensory Neurons of Caenorhabditis elegans. *Genetics* **172**:2239-2252 https://doi.org/10.1534/genetics.105.050013

44. **Hedgecock EM,** Russell RL (1975) Normal and mutant thermotaxis in the nematode Caenorhabditis elegans. *Proc Natl Acad Sci USA* **72**:4061-4065 https://doi.org/10.1073/pnas.72.10.4061

45. **Ryu WS,** Samuel ADT (2002) Thermotaxis in *Caenorhabditis elegans* Analyzed by Measuring Responses to Defined Thermal Stimuli. *J Neurosci* **22**:5727-5733 https://doi.org/10.1523/JNEUROSCI.22-13-05727.2002

46. **Kuhara A,** Ohnishi N, Shimowada T, Mori I (2011) Neural coding in a single sensory neuron controlling opposite seeking behaviours in Caenorhabditis elegans. *Nat Commun* **2** https://doi.org/10.1038/ncomms1352

47. **Mori I,** Ohshima Y (1995) Neural regulation of thermotaxis in Caenorhabditis elegans. *Nature* **376**:344-348 https://doi.org/10.1038/376344a0

48. **Kuhara A,** Mori I (2006) Molecular Physiology of the Neural Circuit for Calcineurin-Dependent Associative Learning in *Caenorhabditis elegans*. *J Neurosci* **26**:9355-9364 https://doi.org/10.1523/JNEUROSCI.0517-06.2006

49. **Hobert O,** D'Alberti T, Liu Y, Ruvkun G (1998) Control of Neural Development and Function in a Thermoregulatory Network by the LIM Homeobox Gene lin-11. *J Neurosci* **18**:2084-2096 https://doi.org/10.1523/JNEUROSCI.18-06-02084.1998

50. **Chung SH,** Clark DA, Gabel CV, Mazur E, Samuel AD (2006) The role of the AFD neuron in C. elegans thermotaxis analyzed using femtosecond laser ablation. *BMC Neurosci* **7** https://doi.org/10.1186/1471-2202-7-30

51. **Ikeda M,** Nakano S, Giles AC, Xu L, Costa WS, Gottschalk A, et al. (2020) Context-dependent operation of neural circuits underlies a navigation behavior in Caenorhabditis elegans. *PNAS* **117**:6178-6188 https://doi.org/10.1073/pnas.1918528117

52. **Han B,** Dong Y, Zhang L, Liu Y, Rabinowitch I, Bai J (2017) Dopamine signaling tunes spatial pattern selectivity in C. elegans. *eLife* **6** https://doi.org/10.7554/eLife.22896

53. **Komatsu H,** Jin Y-H, L'Etoile N, Mori I, Bargmann CI, Akaike N, et al. (1999) Functional reconstitution of a heteromeric cyclic nucleotide-gated channel of Caenorhabditis elegans in cultured cells. *Brain Research* **821**:160-168 https://doi.org/10.1016/S0006-8993(99)01111-7

54. **Finn JT,** Krautwurst D, Schroeder JE, Chen T-Y, Reed RR, Yau K-W (1998) Functional Co-assembly among Subunits of Cyclic-Nucleotide-Activated, Nonselective Cation Channels, and Across Species from Nematode to Human. *Biophysical Journal* **74**:1333-1345 https://doi.org/10.1016/S0006-3495(98)77846-4

55. **Kaupp UB,** Seifert R (2002) Cyclic Nucleotide-Gated Ion Channels. *Physiological Reviews* **82**:769-824 https://doi.org/10.1152/physrev.00008.2002

56. **Xue J,** Han Y, Zeng W, Jiang Y (2022) Structural mechanisms of assembly, permeation, gating, and pharmacology of native human rod CNG channel. *Neuron* **110**:86-95.e5. https://doi.org/10.1016/j.neuron.2021.10.006

57. **Harris G,** Shen Y, Ha H, Donato A, Wallis S, Zhang X, et al. (2014) Dissecting the Signaling Mechanisms Underlying Recognition and Preference of Food Odors. *J Neurosci* **34**:9389-9403 https://doi.org/10.1523/JNEUROSCI.0012-14.2014

58. **He C,** Altshuler-Keylin S, Daniel D, L'Etoile -->Noelle D, O'Halloran D (2016) The cyclic nucleotide gated channel subunit CNG-1 instructs behavioral outputs in Caenorhabditis elegans by coincidence detection of nutritional status and olfactory input. *Neuroscience Letters* **632**:71-78 https://doi.org/10.1016/j.neulet.2016.08.037

59. **Herrero A,** Yoshii T, Ispizua JI, Colque C, Veenstra JA, Muraro NI, et al. (2020) Coupling Neuropeptide Levels to Structural Plasticity in Drosophila Clock Neurons. *Current Biology* **30**:3154-3166.e4. https://doi.org/10.1016/j.cub.2020.06.009

60. **Feketa VV,** Nikolaev YA, Merriman DK, Bagriantsev SN, Gracheva EO (2020) CNGA3 acts as a cold sensor in hypothalamic neurons. Lishko PV, Aldrich RW, Tominaga M, Sobolevsky A, editors. *eLife* **9**:e55370 https://doi.org/10.7554/eLife.55370

61. **Dolzer J,** Schröder K, Stengl M (2021) Cyclic nucleotide-dependent ionic currents in olfactory receptor neurons of the hawkmoth Manduca sexta suggest pull–push sensitivity modulation. *European Journal of Neuroscience* **54**:4804-4826 https://doi.org/10.1111/ejn.15346

62. **Kelliher KR,** Ziesmann J, Munger SD, Reed RR, Zufall F (2003) Importance of the CNGA4 channel gene for odor discrimination and adaptation in behaving mice. *Proceedings of the National Academy of Sciences* **100**:4299-4304 https://doi.org/10.1073/pnas.0736071100

63. **Michalakis S,** Kleppisch T, Polta SA, Wotjak CT, Koch S, Rammes G, et al. (2011) Altered synaptic plasticity and behavioral abnormalities in CNGA3-deficient mice. Genes. *Brain and Behavior* **10**:137-148 https://doi.org/10.1111/j.1601-183X.2010.00646.x

64. **Haverkamp S,** Michalakis S, Claes E, Seeliger MW, Humphries P, Biel M, et al. (2006) Synaptic Plasticity in CNGA3−/− Mice: Cone Bipolar Cells React on the Missing Cone Input and Form Ectopic Synapses with Rods. *J Neurosci* **26**:5248-5255 https://doi.org/10.1523/JNEUROSCI.4483-05.2006

65. **Komatsu H,** Mori I, Rhee J-S, Akaike N, Ohshima Y (1996) Mutations in a Cyclic Nucleotide–Gated Channel Lead to Abnormal Thermosensation and Chemosensation in C. elegans. *Neuron* **17**:707-718 https://doi.org/10.1016/S0896-6273(00)80202-0

66. **Kimura KD,** Miyawaki A, Matsumoto K, Mori I (2004) The *C. elegans* Thermosensory Neuron AFD Responds to Warming. *Current Biology* **14**:1291-1295 https://doi.org/10.1016/j.cub.2004.06.060

67. **Parida L,** Neogi S, Padmanabhan V (2014) Effect of Temperature Pre-Exposure on the Locomotion and Chemotaxis of C. elegans. *PLOS One* **9**:e111342 https://doi.org/10.1371/journal.pone.0111342

68. **Altanbadralt M,** Basutta J, Hajen K, Parmar J, Sidhu BV (2015) The effect of temperature on the speed of locomotion in *Caenorhabditis elegans*. *The Expedition* **5**

69. **Wojtyniak M,** Brear AG, O'Halloran DM, Sengupta P (2013) Cell- and subunit-specific mechanisms of CNG channel ciliary trafficking and localization in C. elegans. *J Cell Sci* **126**:4381-4395 https://doi.org/10.1242/jcs.127274

70. **Hill TJ,** Sengupta P. (2023) Feedforward and feedback mechanisms cooperatively regulate rapid experience-dependent response adaptation in a single thermosensory neuron type. *bioRxiv* https://doi.org/10.1101/2023.12.05.570166

71. **Cho S-W,** Choi KY, Park C-S (2004) A new putative cyclic nucleotide-gated channel gene, cng-3, is critical for thermotolerance in Caenorhabditis elegans. *Biochemical and Biophysical Research Communications* **325**:525-531 https://doi.org/10.1016/j.bbrc.2004.10.060

72. **Kagoshima H,** Kohara Y (2015) Co-expression of the transcription factors CEH-14 and TTX-1 regulates AFD neuron-specific genes gcy-8 and gcy-18 in C. elegans. *Developmental Biology* **399**:325-336 https://doi.org/10.1016/j.ydbio.2015.01.010

73. **He S,** Cuentas-Condori A, Miller DM III (2019) NATF (Native and Tissue-Specific Fluorescence): A Strategy for Bright, Tissue-Specific GFP Labeling of Native Proteins in Caenorhabditis elegans. *Genetics* **212**:387-395 https://doi.org/10.1534/genetics.119.302063

74. **Harris N,** Bates SG, Zhuang Z, Bernstein M, Stonemetz JM, Hill TJ, et al. (2023) Molecular encoding of stimulus features in a single sensory neuron type enables neuronal and behavioral plasticity. *Current Biology* **0** https://doi.org/10.1016/j.cub.2023.02.073

75. **Nguyen PAT,** Liou W, Hall DH, Leroux MR (2014) Ciliopathy proteins establish a bipartite signaling compartment in a C. elegans thermosensory neuron. *Journal of Cell Science* **127**:5317-5330 https://doi.org/10.1242/jcs.157610

76. **Glauser DA,** Chen WC, Agin R, MacInnis BL, Hellman AB, Garrity PA, et al. (2011) Heat Avoidance Is Regulated by Transient Receptor Potential (TRP) Channels and a Neuropeptide Signaling Pathway in Caenorhabditis elegans. *Genetics* **188**:91-103 https://doi.org/10.1534/genetics.111.127100

77. **Árnadóttir J,** O'Hagan R, Chen Y, Goodman MB, Chalfie M (2011) The DEG/ENaC Protein MEC-10 Regulates the Transduction Channel Complex in Caenorhabditis elegans Touch Receptor Neurons. *J Neurosci* **31**:12695-12704

78. **Chatzigeorgiou M,** Grundy L, Kindt KS, Lee W-H, Driscoll M, Schafer WR (2010) Spatial Asymmetry in the Mechanosensory Phenotypes of the C. elegans DEG/ENaC Gene mec-10. *Journal of Neurophysiology* **104**:3334-3344 https://doi.org/10.1152/jn.00330.2010

79. **Huang M,** Chalfie M (1994) Gene interactions affecting mechanosensory transduction in Caenorhabditis elegans. *Nature* **367**:467-470 https://doi.org/10.1038/367467a0

80. **Zhang S,** Ma C, Chalfie M (2004) Combinatorial Marking of Cells and Organelles with Reconstituted Fluorescent Proteins. *Cell* **119**:137-144 https://doi.org/10.1016/j.cell.2004.09.012

81. **Wu J,** Duggan A, Chalfie M (2001) Inhibition of touch cell fate by egl-44 and egl-46 in C. elegans. *Genes Dev* **15**:789-802 https://doi.org/10.1101/gad.857401

82. **Kunitomo H,** Sato H, Iwata R, Satoh Y, Ohno H, Yamada K, et al. (2013) Concentration memory-dependent synaptic plasticity of a taste circuit regulates salt concentration chemotaxis in Caenorhabditis elegans. *Nat Commun* **4**:2210 https://doi.org/10.1038/ncomms3210

83. **Güiza J,** Barría I, Sáez JC, Vega JL. (2018) Innexins: Expression, Regulation, and Functions. *Frontiers in Physiology* **9**:1414 https://doi.org/10.3389/fphys.2018.01414

84. **Altun ZF,** Chen B, Wang Z-W, Hall DH (2009) High resolution map of Caenorhabditis elegans gap junction proteins. *Developmental Dynamics* **238**:1936-1950 https://doi.org/10.1002/dvdy.22025

85. **Phelan P,** Starich TA (2001) Innexins get into the gap. *BioEssays* **23**:388-396 https://doi.org/10.1002/bies.1057

86. **Taylor SR,** Santpere G, Weinreb A, Barrett A, Reilly MB, Xu C, et al. (2021) Molecular topography of an entire nervous system. *Cell* **184**:4329-4347.e23. https://doi.org/10.1016/j.cell.2021.06.023

87. **Rabinowitch I,** Upadhyaya B, Pant A, Galski D, Kreines L, Bai J (2021) Circumventing neural damage in a C. elegans chemosensory circuit using genetically engineered synapses. *Cell Systems* **12**:263-271.e4. https://doi.org/10.1016/j.cels.2020.12.003

88. **Choi M-K,** Liu H, Wu T, Yang W, Zhang Y (2020) NMDAR-mediated modulation of gap junction circuit regulates olfactory learning in C. elegans. *Nat Commun* **11**:3467 https://doi.org/10.1038/s41467-020-17218-0

89. **Rabinowitch I,** Chatzigeorgiou M, Zhao B, Treinin M, Schafer WR (2014) Rewiring neural circuits by the insertion of ectopic electrical synapses in transgenic C. elegans. *Nat Commun* **5**:4442 https://doi.org/10.1038/ncomms5442

90. **Rabinowitch I,** Schafer WR (2015) Engineering new synaptic connections in the C. elegans connectome. *Worm* **4**:e992668 https://doi.org/10.4161/21624054.2014.992668

91. **Chang AJ,** Chronis N, Karow DS, Marletta MA, Bargmann CI (2006) A Distributed Chemosensory Circuit for Oxygen Preference in C. elegans. *PLOS Biology* **4**:e274 https://doi.org/10.1371/journal.pbio.0040274

92. **Hart AC,** Sims S, Kaplan JM (1995) Synaptic code for sensory modalities revealed by C. elegans GLR-1 glutamate receptor. *Nature* **378**:82-85 https://doi.org/10.1038/378082a0

93. **Kaplan JM,** Horvitz HR (1993) A dual mechanosensory and chemosensory neuron in Caenorhabditis elegans. *Proceedings of the National Academy of Sciences* **90**:2227-2231 https://doi.org/10.1073/pnas.90.6.2227

94. **Yoshida K,** Hirotsu T, Tagawa T, Oda S, Wakabayashi T, Iino Y, et al. (2012) Odour concentration-dependent olfactory preference change in C. elegans. *Nat Commun* **3** https://doi.org/10.1038/ncomms1750

95. **Biron D,** Wasserman S, Thomas JH, Samuel ADT, Sengupta P (2008) An olfactory neuron responds stochastically to temperature and modulates Caenorhabditis elegans thermotactic behavior. *Proceedings of the National Academy of Sciences* **105**:11002-11007 https://doi.org/10.1073/pnas.0805004105

96. **Kuhara A,** Okumura M, Kimata T, Tanizawa Y, Takano R, Kimura KD, et al. (2008) Temperature Sensing by an Olfactory Neuron in a Circuit Controlling Behavior of C. elegans. *Science* **320**:803-807 https://doi.org/10.1126/science.1148922

97. **Kano A,** Matsuyama HJ, Nakano S, Mori I (2023) AWC thermosensory neuron interferes with information processing in a compact circuit regulating temperature-evoked posture dynamics in the nematode *Caenorhabditis elegans*. *Neuroscience Research* **188**:10-27 https://doi.org/10.1016/j.neures.2022.11.001

98. **O'Halloran DM,** Altshuler-Keylin S, Zhang X-D, He C, Morales-Phan C, Yu Y, et al. (2017) Contribution of the cyclic nucleotide gated channel subunit, CNG-3, to olfactory plasticity in Caenorhabditis elegans. *Sci Rep* **7** https://doi.org/10.1038/s41598-017-00126-7

99. **Peng C,** Rich ED, Varnum MD (2004) Subunit Configuration of Heteromeric Cone Cyclic Nucleotide-Gated Channels. *Neuron* **42**:401-410 https://doi.org/10.1016/S0896-6273(04)00225-9

100. **Shuart NG,** Haitin Y, Camp SS, Black KD, Zagotta WN (2011) Molecular mechanism for 3:1 subunit stoichiometry of rod cyclic nucleotide-gated ion channels. *Nat Commun* **2** https://doi.org/10.1038/ncomms1466

101. **Zhong H,** Molday LL, Molday RS, Yau K-W (2002) The heteromeric cyclic nucleotide-gated channel adopts a 3A:1B stoichiometry. *Nature* **420**:193-198 https://doi.org/10.1038/nature01201

102. **Coburn CM,** Bargmann CI (1996) A Putative Cyclic Nucleotide–Gated Channel Is Required for Sensory Development and Function in C. elegans. *Neuron* **17**:695-706 https://doi.org/10.1016/S0896-6273(00)80201-9

103. **Yuan C,** Gerhards L, Solov'yov IA, Dedek K (2024) Biotin-cGMP and -cAMP are able to permeate through the gap junctions of some amacrine cells in the mouse retina despite their large size. *Front Ophthalmol* **3** https://doi.org/10.3389/fopht.2023.1334602

104. **Moore KB,** Mitchell CK, Lin Y-P, Lee Y-H, Shihabeddin E, O'Brien J (2020) Localized Calcium Signaling and the Control of Coupling at Cx36 Gap Junctions. *eNeuro* **7** https://doi.org/10.1523/ENEURO.0445-19.2020

105. **Vaughn MJ,** Haas JS (2022) On the Diverse Functions of Electrical Synapses. *Front Cell Neurosci* **16** https://doi.org/10.3389/fncel.2022.910015

106. **Jin EJ,** Park S, Lyu X, Jin Y (2020) Gap junctions: historical discoveries and new findings in the Caenorhabditis elegans nervous system. *Biology Open* **9**:bio053983 https://doi.org/10.1242/bio.053983

107. **Liu S,** Schulze E, Baumeister R (2012) Temperature- and Touch-Sensitive Neurons Couple CNG and TRPV Channel Activities to Control Heat Avoidance in Caenorhabditis elegans. *PLOS One* **7**:e32360 https://doi.org/10.1371/journal.pone.0032360

108. **Brenner S** (1974) The genetics of Caenorhabditis elegans. *Genetics* **77**:71-94 https://doi.org/10.1093/genetics/77.1.71

109. **Rabinowitch I,** Upadhyaya B, Pant A, Galski D, Kreines L, Bai J (2021) Circumventing neural damage in a *C. elegans* chemosensory circuit using genetically engineered synapses. *Cell Systems* **12**:263-271.e4. https://doi.org/10.1016/j.cels.2020.12.003

110. **Frøkjær-Jensen C,** Davis MW, Ailion M, Jorgensen EM (2012) Improved Mos1-mediated transgenesis in C. elegans. *Nat Methods* **9**:117-118 https://doi.org/10.1038/nmeth.1865

111. **Zhang L,** Wang Y, Dong Y, Pant A, Liu Y, Masserman L, et al. (2022) The endophilin curvature-sensitive motif requires electrostatic guidance to recycle synaptic vesicles in vivo. *Developmental Cell* **57**:750-766.e5. https://doi.org/10.1016/j.devcel.2022.02.021

112. **Ghanta KS,** Ishidate T, Mello CC (2021) Microinjection for precision genome editing in *Caenorhabditis elegans*. *STAR Protocols* **2** https://doi.org/10.1016/j.xpro.2021.100748

113. **Paix A,** Folkmann A, Rasoloson D, Seydoux G. (2015) High Efficiency, Homology-Directed Genome Editing in Caenorhabditis elegans Using CRISPR-Cas9 Ribonucleoprotein Complexes. *Genetics* **201**:47-54 https://doi.org/10.1534/genetics.115.179382

114. **He S,** Cuentas-Condori A, Miller DM (2019) NATF (Native and Tissue-Specific Fluorescence): A Strategy for Bright, Tissue-Specific GFP Labeling of Native Proteins in Caenorhabditis elegans. *Genetics* **212**:387-395 https://doi.org/10.1534/genetics.119.302063

Rosero M, Bai J (2026) AFD Thermosensory Neurons mediate tactile-dependent Locomotion modulation in C. Elegans. Dryad Digital Repository. https://doi.org/10.5061/dryad.k3j9kd5pz

Peer reviews

Reviewer #1 (Public review):

Summary:

In this manuscript, Rosero and Bai examined how the well-known thermosensory neuron in C. elegans, AFD, regulates context-dependent locomotory behavior based on the tactile experience. Here they show that AFD uses discrete cGMP signalling molecules and independent of its dendritic sensory endings regulates this locomotory behavior. The authors also show here that AFD's connection to one of the hub interneurons, AIB, through gap junction/electrical synapses, is necessary and sufficient for the regulation of this context-dependent locomotion modulation.

Strengths:

This is an interesting paper showcasing how a sensory neuron in C. elegans can employ a distinct set of molecular strategies and different physical parts to regulate a completely distinct set of behaviors, which were not been shown to be regulated by AFD before. The experiments were well performed and the results are clear. However, there are some questions about the mechanism of this regulation. This reviewer thinks that the authors should address these concerns before the final published version of this manuscript.

Comments on revisions:

In this revised manuscript, Rosero and Bai satisfactorily addressed all the concerns raised by this reviewer regarding their original manuscript. This reviewer appreciates the authors' effort. This revised and improved manuscript demonstrates that a sensory neuron in C. elegans can utilize distinct molecular strategies and circuit engagements to regulate distinct sets of behaviors. This reviewer believes that the manuscript is suitable for final acceptance in eLife.

https://doi.org/10.7554/eLife.106496.2.sa3

Reviewer #2 (Public review):

The goal of the study was to uncover the mechanisms mediating tactile-context-dependent locomotion modulation in C. elegans, which represents an interesting model of behavioral plasticity. Starting from a candidate genetic screen focusing on guanylate cyclase (GCY) mutants, the authors identified the AFD-specific gcy-18 gene as essential for tactile-context-dependent locomotion modulation. AFD has been primarily characterized as a thermosensory neuron. However, key thermosensory transduction genes and the sensory ending structure of AFD were shown here to be dispensable for tactile-context locomotion modulation. AFD actuates tactile-context locomotion modulation via the cell-autonomous

actions of GCY-18 and the CNG-3 cyclic nucleotide-gated channel, and via AFD's connection with AIB interneurons through electrical synapses. At the circuit level, AIB also receive inputs from the mechanosensory neuron FLP, which was also shown to be relevant for tactile-context-dependent locomotion modulation.

For this study, the authors combined a very clever microfluidic-based behavioral assay with a large set of genetic manipulations to dissect the molecular and cellular pathways involved. Rescue experiments with single-copy transgenes are particularly convincing. The study is very clearly written, and the figures are nicely illustrated with diagrams that effectively convey the authors' interpretation. Overall, the convergence of behavioral assays, genetics, and circuit analysis provides convincing support for the proposed role of the AFD-AIB connection, potentially downstream of FLP via synapic and of other mechanosensory neurons via extra-synaptic communication.

The facts that AFD mediates tactile-context locomotion modulation, that this role relies on GCY-18, and on electrical synapses linking AFD to AIB are new, somewhat unexpected, and interesting. The study raises intriguing and addressable questions about the role of innexin-based cellular communication in a multimodal sensory-behavior microcircuit, including the direction and nature of the signal(s) transmitted through these electrical synapses. These questions remain difficult to address in most experimental systems. The compact and genetically tractable nervous system of C. elegans provides a powerful entry point for addressing them in the context of an intact in vivo circuit.

https://doi.org/10.7554/eLife.106496.2.sa2

Reviewer #3 (Public review):

Summary:

Rosero and Bai report an unconventional role of AFD neurons in mediating tactile-dependent locomotion modulation, independent of their well-established thermosensory function. They partially elucidate the signaling mechanisms underlying this AFD-dependent behavioral modulation. The regulation does not require the sensory dendritic endings of AFD but rather the AFD neurons themselves. This process involves a distinct set of cGMP signaling proteins and CNG channel subunits separate from those involved in thermosensation or thermotaxis. Furthermore, the authors demonstrate that AIB interneurons connect AFD to mechanosensory circuits through electrical synapses. They conclude that, beyond its primary function in thermosensation, AFD contributes to context-dependent neuroplasticity and behavioral modulation via broader circuit connectivity.

While the discovery of multifunctionality in AFD is not entirely unexpected, given the limited number of neurons in C. elegans (302 in total), the molecular and cellular mechanisms underlying this AFD-dependent behavioral modulation, as revealed in this study, provide valuable insights into the field.

Strengths:

(1) The authors uncover a novel role of AFD neurons in mediating tactile-dependent locomotion modulation, distinct from their well-established thermosensory function, providing an important conceptual contribution to our understanding of how individual neurons can support multiple, mechanistically separable behavioral functions.

(2) They provide meaningful mechanistic insight into how AFD, GCY-18-dependent cGMP signaling, and AFD-AIB electrical coupling contribute to this AFD-dependent behavioral modulation.

(3) The neural behavior assays utilizing two types of microfluidic chambers (uniform and binary chambers) are innovative and well-designed. In the revised manuscript the authors introduce a removable-barrier assay that physically separates exploration and assay phases. This independent behavioral approach addresses prior concerns about ongoing sensory input and confirms that tactile experience alone is sufficient to modulate locomotion.

(4) By comparing AFD's role in locomotion modulation to its thermosensory function throughout the study, the authors present strong evidence supporting these as two independent functions of AFD.

(5) The finding that AFD contributes to context-dependent behavioral modulation is significant, further reinforcing the growing evidence that individual neurons can serve multiple functions through broader circuit connectivity.

Weaknesses:

While the requirement for AFD, GCY-18, and AFD-AIB electrical coupling is well supported, the directionality of information flow and the precise mode of interaction between mechanosensory neurons, AIB, and AFD remain unclear and an area of future studies.

Overall, the authors successfully achieve their primary aim of identifying and characterizing a novel role for AFD in tactile experience-dependent locomotion modulation. This work contributes meaningfully to the growing body of literature demonstrating multifunctionality and context-dependent reconfiguration of individual neurons within compact nervous systems.

https://doi.org/10.7554/eLife.106496.2.sa1

Author Response:

The following is the authors' response to the original reviews.

> ***Public Reviews:***
>
> *Although the reviewers agree on the potential importance of this study, they have brought out multiple pertinent queries with respect to the interpretation of some of the results presented in the manuscript, that the authors should consider addressing. The reviewers have also suggested modifications that would increase the clarity of the manuscript.*

We appreciate the thoughtful evaluation of our manuscript by the reviewers and the editor. We are encouraged by their recognition of the importance of our study and have carefully considered all the points raised. In response, we have added new data and revised the text to address the concerns and improve the clarity of the manuscript. Our detailed responses to the reviewers' comments are provided below.

> ***Reviewer #1 (Public review):***
>
> *Summary:*
>
> *In this manuscript, Rosero and Bai examined how the well-known thermosensory neuron in C. elegans, AFD, regulates context-dependent locomotory behavior based on the tactile experience. Here they show that AFD uses discrete cGMP signaling molecules and independent of its dendritic sensory endings regulates this locomotory behavior. The authors also show here that AFD's connection to one of the hub interneurons, AIB, through gap junction/electrical synapses, is necessary and sufficient for the regulation of this context-dependent locomotion modulation.*

Strengths:

This is an interesting paper showcasing how a sensory neuron in C. elegans can employ a distinct set of molecular strategies and different physical parts to regulate a completely distinct set of behaviors, which were not been shown to be regulated by AFD before. The experiments were well performed and the results are clear. However, there are some questions about the mechanism of this regulation. This reviewer thinks that the authors should address these concerns before the final published version of this manuscript.

Weaknesses:

(1) The authors argued about the role of prior exposure to different physical contexts which might be responsible for the difference in their locomotory behavior. However, the worms in the binary chamber (with both non-uniformly sized and spaced pillars) experienced both sets of pillars for one hour prior to the assay and they were also free to move between two sets of environments during the assay. So, this is not completely a switch between two different types of tactile barriers (or not completely restricted to prior experience), but rather a difference between experiencing a more complex environment vs a simple uniform environment. They should rephrase their findings. To strictly argue about the prior experience, the authors need to somehow restrict the worms from entering the uniform assay zone during the 1hr training period.

We agree that, in the original design, worms in the binary chamber experience a more complex physical environment while retaining access to both exploration and assay zones. We have therefore revised the manuscript to more clearly distinguish between behavioral differences due to exposure to a complex environment and modulation driven by prior experience.

To directly test whether locomotion modulation can be sustained by prior physical experience in the absence of continued access to the exploration zone, we introduced a barrier-based assay that prevents worms from re-entering the exploration zone before locomotion is measured. The results section has been revised accordingly to explicitly address this point.

Revisions to the manuscript:

Lines 122-139: Added two paragraphs describing the new assay and summarizing the corresponding results.

“Because worms in the binary chamber are exposed to both pillar types and remain free to move between exploration and assay zones, the behavioral differences described above could reflect exposure to a more complex physical environment rather than prior experience alone. To directly test whether locomotion is modulated by prior physical experience independently of continued access to the exploration zone, we designed microfluidic chambers in which the assay zone could be separated from the exploration zone by a removable barrier (Fig. 1–Supplement 1A). In these chambers, worms were initially allowed to explore the entire device, including exploration zones that either matched or differed from the assay zone. A barrier was then inserted to prevent worms in the assay zone from re-entering the exploration zones.

Under these conditions, locomotion immediately after barrier insertion was higher in worms that had previously explored physical settings matching the assay zone (205 ± 8 μm/s) than in worms that had explored non-matching settings (151 ± 7 μm/s; p = 0.006; Fig. 1–Supplement 1B). This difference persisted when worms were recorded 40 minutes after barrier insertion, with animals in matching chamber retaining their higher locomotion rates (218 ± 11 μm/s) compared to those in non-matching chambers (185 ± 8 μm/s; p = 0.02; Fig. 1–Supplement 1B).

These findings demonstrate that prior exploration of distinct physical environments can modulate locomotion even when worms are prevented from returning to those environments, supporting a role for prior physical experience independent of ongoing sensory input."

Figure 1–Supplement 1: New figure showing the experimental design and behavioral results.

> *(2) The authors here argued that the sensory endings of AFD are not required for this novel role of AFD in context-dependent locomotion modulation. However, gcy-18 has been shown to be exclusively localized to the ciliated sensory endings of AFD and even misexpression of GCY-18 in other sensory neurons also leads to localizations in sensory endings (Nguyen et. al., 2014 and Takeishi et. al., 2016). They should check whether gcy-18 or tax-2 gets mislocalized in kcc-3 or tax-1 mutants.*

As the reviewer suggested, we examined GCY-18 localization in wild type animals and in mutants with defective sensory microvilli using a split-GFP strategy (He et al., 2019). We generated a *gcy18::gfp11×7* knock-in strain using CRISPR–Cas9 to visualize endogenous GCY-18 localization. Consistent with prior studies, GCY-18 localized strongly to the AFD dendritic ending in wild-type animals (Figure 4– Supplement 1A, A', A''), with an additional weaker signal detectable near the soma and axon (Figure 4– Supplement 1A''').

In *kcc-3* mutants, GCY-18 remained localized to the distal dendrite despite disruption of sensory microvillar morphology (Figure 4–Supplement 1B–B''). Similarly, in *ttx-1* mutants, which completely lack AFD sensory microvilli, GCY-18 still localized to the distal dendrite (Figure 4–Supplement 1C–C'') and remained detectable near the soma and axon (Figure 4–Supplement 1C''').

In the revised manuscript, we clarify both the implications and the limitations of these imaging experiments, noting that "although these experiments do not identify the precise subcellular site at which GCY-18 acts, they show that disruption of sensory microvilli does not substantially alter GCY-18 localization within AFD." The exact site at which GCY-18 functions to support locomotion modulation therefore remains an important open question for future investigation.

Revisions to the manuscript:

Figure 4-Supplement 1: Added a new figure reporting GCY-18 localization in wild type and mutant worms.

Lines 268-280: Added a new paragraph reporting GCY-18 localization in wild type, *kcc-3*, and *ttx-1* mutants and clarifying its relevance to the reviewer's concern.

"Given that *gcy-18* is required for context-dependent locomotion modulation and that GCY-18 localizes to the distal dendrite of AFD, we next examined how disruption of sensory microvilli affects its localization in AFD. We used a split-GFP strategy to visualize endogenous GCY-18 [73]. A tandem array of seven GFP11 β-strands (GFP11x7) was inserted at the C-terminus of GCY-18 using CRISPR-Cas9. When complemented with GFP1-10, GCY-18::GFP11x7 fluorescence was strongly enriched at the AFD sensory microvilli near the nose (Fig. 4–Supplement 1A-A''), consistent with previous reports [42,74,75]. In addition, weaker but reproducible GCY-18 signal was detected near the AFD soma and axon (Fig. 4–Supplement 1A'' '). Importantly, in *kcc-3*, which exhibit disrupted sensory microvilli, and *ttx-1* mutants, which lack sensory microvilli, GCY-18 remained localized to the distal dendrite and was still detectable near the soma and axon (Fig. 4–Supplement 1B-B''' and 1C-C'''). Although these experiments do not identify the precise subcellular site at which GCY-18 acts, they show that disruption or loss of sensory microvilli does not substantially alter GCY-18 localization within AFD."

> *(3) MEC-10 was shown to be required for physical space preference through its action in FLP and not the TRNs (PMID: 28349862). Since FLP is involved in harsh touch sensation while TRNs are involved in gentle touch sensation, which are the neuron types responsible for tactile sensation in the assay arena? Does mec-10 rescue in TRNs rescue the phenotype in the current paper?*

We performed cell-specific rescue experiments of *mec-10*. Single-copy expression of *mec-10* cDNA in either FLP neurons alone (*egl-44p*) or TRNs alone (*mec-18p*) did not restore context-dependent locomotion modulation (Fig. 5A). In contrast, co-expression in both FLP and TRNs (*egl-44p::mec-10* + *mec18p::mec-10*), as well as expression from the *mec-10* promoter, rescued the phenotype.

These results indicate that input from multiple *mec-10*-expressing neurons, including both FLP and TRNs, is required for context-dependent locomotion adjustment. This requirement differs from spatial preference behavior, where *mec-10* acts specifically in FLP (Han et al., 2017), suggesting distinct mechanosensory circuits are engaged by different tactile-driven behaviors.

Revisions to the manuscript:

Fig. 5A: Updated to include the cell-specific rescue data.

Lines 317-331: Added a new paragraph describing these findings.

"The *mec-10* gene is expressed in several mechanosensory neurons, including the six touch receptor neurons (TRNs) and the polymodal nociceptors FLP and PVD [77,79]. To determine which neurons are required for tactile-dependent locomotion modulation, we expressed *mec-10* cDNA under cell-specific promoters: *mec-18p* (TRNs) [80], *egl-44p* (FLP) [81], or *mec-10p* (TRNs, FLP, and PVD) [79]. Expression in either FLP or TRNs alone did not restore modulation, as worms carrying *egl-44p::mec-10* (Δspeed: -11± 4%) or *mec-18p::mec-10* (Δspeed: -13 ± 4%) transgenes showed significantly reduced Δspeed compared to wild type (Δ speed: N2: 33 ± 6%; $p < 0.0001$ for both; Fig. 5A). By contrast, *mec-10* co-expression in both FLP and TRNs (Δspeed: 16 ± 4%), or expression from the *mec-10* promoter (Δspeed: 23 ± 4%), restored Δ speed to wild type levels ($p = 0.20$ and $p = 0.57$, respectively; Fig. 5A). These findings indicate that *mec10* expression across multiple mechanosensory neuron types is required for context-dependent locomotion modulation. It is also worth noting that, while both tactile-dependent locomotion modulation and previously reported spatial preference require FLP, only the former depends on TRNs. Together, these findings suggest that distinct subsets of mechanosensory neurons differentially contribute to behaviors shaped by tactile experience."

> *(4) The authors mention that the most direct link between TRNs and AFD is through AIB, but as far as I understand, there are no reports to suggest synapses between TRNs and AIB. However, FLP and AIB are connected through both chemical and electrical synapses, which would make more sense as per their mec10 data. (the authors mentioned about the FLP-AIB-AFD circuit in their discussion but talked about TRNs as the sensory modality). mec-10 rescue experiment in TRNs would clarify this ambiguity.*

We agree with the reviewer that there are no reported synapses between TRNs and AIB, and we have revised Fig. 5 and the corresponding text to clarify this point. In the revised manuscript, we removed any implication of a direct TRN-AIB connection and instead focus on the established FLP-AIB-AFD pathway, while considering potential indirect contributions from TRNs.

As the reviewer suggested, we performed cell-specific *mec-10* rescue experiments. Expression of *mec-10* in either FLP alone or TRNs alone was insufficient to restore tactile-dependent locomotion modulation, whereas co-expression in both cell types rescued the phenotype

(revised Fig. 5A). These results indicate that FLP is essential for this behavior, consistent with the known FLP-AIB-AFD connectivity, and that TRNs are also required.

Given that TRNs lack direct synapses with AIB, TRN requirement suggests the involvement of indirect communication, likely mediated through modulatory mechanisms such as neuropeptide signaling. Accordingly, we have revised the model (revised Fig. 5C) and the corresponding text to clarify that tactiledependent locomotion modulation integrates inputs from multiple *mec-10*-expressing neurons and does not rely on a direct TRN-AIB synaptic connection.

Revisions to the manuscript:

Lines 334–345: Revised paragraph to clarify circuit logic and remove implication of direct TRN-AIB synapses.

"Touch-sensitive neurons that express *mec-10*, including TRNs, FLP, and PVD, do not form direct synapses with AFD, suggesting that tactile information is relayed through intermediary neurons. Because the interneuron AIB receives synaptic input from FLP and forms electrical synapses with AFD, we hypothesized that AIB could serve as a conduit for mechanosensory signals to reach AFD. To test whether AIB is required for tactile-dependent modulation, we examined locomotion in worms with genetically ablated AIB neurons using *npr-9p::caspase* expression [82]. AIB-ablated worms failed to adjust locomotion speed, showing a near-complete loss of modulation (Δspeed: -1 ± 5%) compared to wild type (30 ± 8%, p = 0.001, Fig. 5B). These results demonstrate that AIB is required for AFD-mediated tactile-dependent locomotion modulation. However, because *mec-10*-expressing TRNs are also required, additional pathways beyond AIB likely contribute to transmitting tactile information to AFD, potentially involving indirect synaptic connections through other interneurons or long-distance signaling via neuropeptides or other modulators (Fig. 5C)."

Fig. 5: Updated to include new cell-specific *mec-10* rescue data and revised model.

> *(5) Do inx-7 or inx-10 rescue in AFD and AIB using cell-specific promoters rescue the behavior?*

Yes. We tested this during revision. Using the AFD-specific *srtx-1b* promoter, we expressed *inx10* cDNA selectively in AFD neurons of *inx-10* mutant worms. This manipulation significantly restored tactile-dependent locomotion modulation compared to non-transgenic *inx-10* mutants (Fig. 6D), demonstrating that *inx-10* expression in AFD alone is sufficient to rescue the behavioral defect.

Revisions to the manuscript:

Line 366-370: Added a description of the AFD-specific *inx-10* rescue results.

"We next tested whether restoring *inx-10* specifically in AFD would be sufficient to rescue the behavioral defect. Using the AFD-specific *srtx-1b* promoter, we expressed *inx-10* cDNA in *inx-10* mutant worms. These transgenic animals displayed significantly improved locomotion modulation (Δspeed: 42 ± 5%) compared to non-transgenic *inx-10* mutants (15 ± 4%; p = 0.018; Fig. 6D), indicating that *inx-10* expression in AFD alone is sufficient to restore function."

Fig. 6D: Updated to include new cell-specific *inx-10* rescue data.

> *(6) How Guanylyl cyclase gcy-18 function is related to the electrical synapse activity between AFD and AIB? Is AFD downstream or upstream of AIB in this context?*

At present, the precise relationship between GCY-18 signaling and the AFD-AIB electrical synapse is not fully resolved. Given that AIB receives mechanosensory input from FLP, it is likely that AIB acts upstream of AFD during tactile-dependent locomotion modulation.

However, because the AIB-AFD connection is mediated by gap junctions, communication could also be bi-directional, especially since small signaling molecules such as cGMP and Ca^{2+} are known to diffuse through electrical synapses.

We have therefore revised the manuscript to state explicitly that the directionality of information flow between AFD and AIB remains open, and that this will be an important question for future investigation (Line 455-458).

“Together, these findings support a model in which AIB functions as a hub neuron that relays mechanosensory input from FLP to AFD to modulate locomotion (Fig. 5C). However, because electrical synapses are often bidirectional, information flow may also occur in the opposite direction, from AFD to AIB.”

> ***Reviewer #2 (Public review):***
>
> *Summary:*
>
> *The goal of the study was to uncover the mechanisms mediating tactile-context-dependent locomotion modulation in C. elegans, which represents an interesting model of behavioral plasticity. Starting from a candidate genetic screen focusing on guanylate cyclase (GCY) mutants, the authors identified the AFDspecific gcy-18 gene as essential for tactile-context-dependent locomotion modulation. AFD is primarily characterized as a thermo-sensory neuron. However, key thermosensory transduction genes and the sensory ending structure of AFD were shown here to be dispensable for tactile-context locomotion modulation. AFD actuates tactile-context locomotion modulation via the cell-autonomous actions of GCY-18 and the CNG-3 cyclic nucleotide-gated channel, and via AFD's connection with AIB interneurons through electrical synapses. This represents a potentially relevant synaptic connection linking AFD to the mechanosensory-behavior circuit.*
>
> *Strengths:*
>
> *(1) The fact that AFD mediates tactile-context locomotion modulation is new, rather surprising, and interesting.*
>
> *(2) The authors have combined a very clever microfluidic-based behavioral assay with a large set of genetic manipulations to dissect the molecular and cellular pathways involved. Rescue experiments with singlecopy transgenes are very convincing.*
>
> *(3) The study is very clearly written, and figures are nicely illustrated with diagrams that effectively convey the authors' interpretation.*
>
> *Weaknesses:*
>
> *(1) Whereas GCY-18 in AFD and the AFD-AIB synaptic connection clearly play a role in tactile-context locomotion modulation, whether and how they actually modulate the mechanosensory circuit and/or locomotion circuit remains unclear. The possibility of non-synaptic communication linking mechanosensory neurons and AFD (in either direction) was not explored. Thus, in the end, we have not learned much about what GCY-18 and the AFD-AIB module are doing to actuate tactile context-dependent locomotion modulation.*

We agree with the reviewer that although GCY-18 in AFD and the AFD-AIB connection are clearly required for tactile context-dependent locomotion modulation, the precise mechanisms by which they influence mechanosensory and locomotor circuits remain unresolved. In particular, the possibility of nonsynaptic communication or bidirectional signaling between mechanosensory neurons and AFD cannot be addressed by the current experiments and warrants future investigation.

At the same time, we believe this study reveals several previously unrecognized aspects of tactiledependent locomotion modulation that provide a foundation for future mechanistic investigation.

Specifically, we show that (i) GCY-18 functions in AFD to support tactile-dependent locomotion modulation; (ii) the cGMP-gated channel TAX-4, required for thermosensation, is dispensable for this process, whereas CNG-3 is required, revealing functional specialization within AFD; (iii) the interneuron AIB is necessary for this modulation; and (iv) restoring a single electrical connection between AFD and AIB using mammalian Cx36 is sufficient to rescue tactile-dependent modulation in innexin mutants.

Accordingly, we now explicitly state in the revised Discussion that "a limitation of this study is that the directionality and mode of information flow between AFD and AIB remain unresolved, and defining this relationship will be an important goal for future investigation" (Line 472-475).

> *(2) The authors only focused on speed readout, and we don't know if the many behavioral parameters that are modulated by tactile context are also under the control of AFD-mediated modulation.*

We used locomotion speed as the primary behavioral readout because it provides a robust measure for detecting whether behavior is modified by prior tactile experience, rather than to capture the full spectrum of motor outputs. This strategy is often used to assess experience-dependent behavioral plasticity across sensory modalities and enabled us to uncover the unexpected role of AFD in tactile-dependent plasticity.

In the revised manuscript, we expanded our analysis to include additional behavioral parameters. As described in the Results, AFD-ablated worms showed a complete loss of context-dependent modulation not only in speed, but also in idle time and turning frequency, with no detectable differences between uniform and binary chambers (Fig. 4E). These data strengthen the conclusion that AFD broadly supports tactiledependent behavioral modulation rather than selectively affecting a single locomotor parameter.

Revisions to the manuscript:

Fig. 4E: Revised panel to include additional locomotion parameters, including idle time and turning frequency, in wild type and AFD-ablated worms.

Lines 283–285: Expanded the results to describe changes in locomotion speed, idle time, or turning frequency of AFD-ablated mutant worms. "These animals showed no detectable differences between uniform and binary chambers in locomotion speed, idle time, or turning frequency (Fig. 4E)."

> *(3) The AFD-AIB gap junction reconstruction experiment was conducted in an innexin double mutant background, in which the whole nervous system's functioning might be severely impaired, and its results should be interpreted with this limitation in mind.*

We appreciate the reviewer's concern that the innexin double-mutant background may broadly affect nervous system function, and we agree that loss of innexins is not restricted to the AFD-AIB synapse and could introduce global circuit perturbations.

Importantly, however, the specificity of the rescue is informative. In an *innexin* double-mutant background, where electrical coupling is broadly disrupted, re-establishing a single electrical synapse between AFD and AIB using Cx36 was sufficient to restore tactile-dependent locomotion modulation (Fig. 6D). The ability of a targeted AFD-AIB connection to rescue behavior despite the absence of many other electrical synapses argues against a purely global network defect and instead identifies the AFD-AIB electrical synapse as a critical locus for this modulation.

To further address this concern, we performed an additional rescue experiment in a less perturbed genetic background. In the revised manuscript, we show that AFD-specific expression of *inx-10* rescues locomotion modulation in *inx-10* single mutants (Fig. 6D). Together, these complementary rescue approaches, one restoring endogenous innexin function in AFD and the other reconstituting an electrical synapse using Cx36, support the conclusion that AFD-AIB electrical coupling is sufficient to enable tactile-dependent locomotion modulation, rather than reflecting nonspecific recovery of global circuit function.

Revision to the manuscript:

Fig. 6D and Lines 366-370: Added new data and revised text showing that AFD-specific *inx-10* expression restores tactile-dependent locomotion modulation.

"We next tested whether restoring *inx-10* specifically in AFD would be sufficient to rescue the behavioral defect. Using the AFD-specific *srtx-1b* promoter, we expressed *inx-10* cDNA in *inx-10* mutant worms. These transgenic animals displayed significantly improved locomotion modulation (Δspeed: 42 ± 5%) compared to non-transgenic *inx-10* mutants (15 ± 4%; p = 0.018; Fig. 6D), indicating that *inx-10* expression in AFD alone is sufficient to restore function."

> ***Reviewer #3 (Public review):***
>
> *Summary:*
>
> *Rosero and Bai report an unconventional role of AFD neurons in mediating tactile-dependent locomotion modulation, independent of their well-established thermosensory function. They partially elucidate the signaling mechanisms underlying this AFD-dependent behavioral modulation. The regulation does not require the sensory dendritic endings of AFD but rather the AFD neurons themselves. This process involves a distinct set of cGMP signaling proteins and CNG channel subunits separate from those involved in thermosensation or thermotaxis. Furthermore, the authors demonstrate that AIB interneurons connect AFD to mechanosensory circuits through electrical synapses. They conclude that, beyond its primary function in thermosensation, AFD contributes to context-dependent neuroplasticity and behavioral modulation via broader circuit connectivity.*
>
> *While the discovery of multifunctionality in AFD is not entirely unexpected, given the limited number of neurons in C. elegans (302 in total), the molecular and cellular mechanisms underlying this AFD-dependent behavioral modulation, as revealed in this study, provide valuable insights into the field.*
>
> *Strengths:*
>
> *(1) The authors uncover a novel role of AFD neurons in mediating tactile-dependent locomotion modulation, distinct from their well-established thermosensory function.*

> *(2) They provide partial insights into the signaling mechanisms underlying this AFD-dependent behavioral modulation.*
>
> *(3) The neural behavior assays utilizing two types of microfluidic chambers (uniform and binary chambers) are innovative and well-designed.*
>
> *(4) By comparing AFD's role in locomotion modulation to its thermosensory function throughout the study, the authors present strong evidence supporting these as two independent functions of AFD.*
>
> *(5) The finding that AFD contributes to context-dependent behavioral modulation is significant, further reinforcing the growing evidence that individual neurons can serve multiple functions through broader circuit connectivity.*
>
> *Weaknesses:*
>
> *(1) Limited Behavioral Assays: The study relies solely on neural behavior assays conducted using two types of microfluidic chambers (uniform and binary chambers) to assess context-dependent locomotion modulation. No additional behavioral assays were performed. To strengthen the conclusions, the authors should validate their findings using an independent method, at the very least by testing AFD-ablated animals and gcy-18 mutants with a second behavioral approach.*

The reviewer points out that the original study relied on locomotion assays in two microfluidic environments (uniform and binary chambers) and suggests validation using an independent behavioral approach, particularly for AFD-ablated animals and *gcy-18* mutants.

To address this concern, we developed an independent behavioral assay in which the exploration and assay environments are physically separated by a removable barrier (Figure 1–Supplement 1A). In this design, worms first explored distinct physical settings, after which a barrier was inserted to confine them to an identical assay zone. This approach allowed us to directly test whether context-dependent locomotion modulation can be maintained when worms are prevented from re-entering the exploration environment and must rely solely on prior experience.

Using this assay, we found that wild-type worms that had previously explored environments matching the assay zone moved significantly faster than those that had explored non-matching environments (Figure 1– Supplement 1B-C). These results demonstrate that context-dependent locomotion modulation is retained even when ongoing sensory input from the exploration zone is eliminated, independently validating our original findings using a distinct behavioral paradigm.

Further, using this same assay, we found that locomotion modulation was significantly impaired in both *gcy-18* mutants and AFD-ablated worms (Figure 4–Supplement 2A). Together, these results provide independent behavioral evidence supporting the conclusion that AFD and *gcy-18* are required for contextdependent locomotion modulation.

Revision to the manuscript:

Figure 1–Supplement 1A: Added schematic and results from the removable-barrier assay in wild type animals.

Lines 120-137: Added corresponding Results text describing the new assay and wild-type behavior.

“Because worms in the binary chamber are exposed to both pillar types and remain free to move between exploration and assay zones, the behavioral differences described above could

reflect exposure to a more complex physical environment rather than prior experience alone. To directly test whether locomotion is modulated by prior physical experience independently of continued access to the exploration zone, we designed microfluidic chambers in which the assay zone could be separated from the exploration zone by a removable barrier (Fig. 1–Supplement 1A). In these chambers, worms were initially allowed to explore the entire device, including exploration zones that either matched or differed from the assay zone. A barrier was then inserted to prevent worms in the assay zone from re-entering the exploration zones.

Under these conditions, locomotion immediately after barrier insertion was higher in worms that had previously explored physical settings matching the assay zone (205 ± 8 μm/s) than in worms that had explored non-matching settings (151 ± 7 μm/s; p = 0.006; Fig. 1–Supplement 1B). This difference persisted when worms were recorded 40 minutes after barrier insertion, with animals in matching chamber retaining their higher locomotion rates (218 ± 11 μm/s) compared to those in non-matching chambers (185 ± 8 μm/s; p = 0.02; Fig. 1–Supplement 1B). These findings demonstrate that prior exploration of distinct physical environments can modulate locomotion even when worms are prevented from returning to those environments, supporting a role for prior physical experience independent of ongoing sensory input." Figure 4–Supplement 2A: Added data for *gcy-18* mutants and AFD-ablated worms in the removable barrier assay.

Lines 288-296: Added text describing behavioral defects in *gcy-18* mutants and AFD-ablated worms using the new assay.

"Building on our finding that locomotion modulation can be driven by prior physical experience even after worms are prevented from re-entering the exploration zones, we next tested whether AFD is required for this modulation using chambers in which the exploration and assay zones were separated by a removable barrier (Fig. 1–Supplement 1A). Under these conditions, locomotion modulation was significantly reduced in AFD-ablated worms (Δspeed: -AFD = 1 ± 6% vs. N2 = 23 ± 7%; p = 0.036; Fig. 4–Supplement 2A). Similarly, *gcy-18* mutants showed defective locomotion modulation (Δspeed: *gcy-18* = -1 ± 8% vs. N2 = 23 ± 7%; p = 0.034; Fig. 4–Supplement 2A). These results indicate that AFD and *gcy-18* are required to generate locomotion modulation in response to recent physical experience, even when continued access to surrounding environments is restricted."

> *(2) Clarity in Behavioral Assay Methodology: The methodology for conducting the behavioral assays is unclear. It appears that worms were free to move between the exploration and assay zones, with no control over the duration each worm spent in either zone. This lack of regulation may introduce variability in tactile experience across individuals, potentially affecting the reproducibility and quantitativeness of the method. The authors should clarify whether and how they accounted for this variability.*

In the primary assay, worms were allowed to move freely between the exploration and assay zones for one hour, and each animal's tactile experience depended on its exploratory trajectory. To address the resulting variability, we performed an a *priori* power analysis, which determined that approximately 160 worms distributed across more than 20 chambers per condition were sufficient to obtain reliable populationlevel measurements. This sampling strategy was applied consistently across all experiments. Accordingly, analyses emphasize well-powered population means rather than individual trajectories, ensuring robust and reproducible comparisons despite variability in individual experience.

In addition, as described above, we developed a removable-barrier assay that eliminates variability from ongoing exploration by confining worms to the assay zone after a defined exploration period. The consistency of behavioral effects across both assays further supports the robustness and reproducibility of the approach.

> *(3) Potential Developmental and Behavioral Confounds in Mutant Analysis: Several neuronal mutant strains were used in this study, yet the effects of these mutations on development and general behavior (e.g., movement ability) were not discussed. Although young adult worms were used for behavioral assays, were they at similar biological ages? To rule out confounding factors, locomotion assays assessing movement ability should be conducted (see reference PMID 25561524).*

To address the possibility that behavioral phenotypes in mutant strains arise from developmental defects or impaired general locomotion, we directly measured locomotion speed on agar plates and body length in *gcy-18* mutant and AFD-ablated worms. Neither genotype showed defects in basal locomotion speed or body length compared to wild type animals (Figure 4–Supplement 2B-C), indicating that the observed modulation defects are not explained by impaired development or gross motor ability.

To further control for developmental variability, all behavioral assays were performed using agesynchronized populations. Animals were selected at a defined gravid adult stage, identified by the presence of 5-10 eggs arranged in a single row within the gonad. All mutant strains reached this developmental stage approximately three days after egg laying, comparable to wild type animals.

Revision to the manuscript:

Figure 4–Supplement 2B-C: Added quantification of locomotion speed on agar plates and body length for *gcy-18* mutants and AFD-ablated worms.

Lines 297-304: Added text describing the data presented in Figure 4–Supplement 2B-C.

“Finally, to determine whether the modulation defects observed in *gcy-18* mutants and AFD-ablated worms could be attributed to developmental abnormalities or gross motor impairments, we measured locomotion speed and body length on standard NGM plates. Both day-1 adult AFD-ablated worms (speed: 281 ± 10 μm/s; p = 0.33; body length: 1.12 ± 0.01 mm; p = 0.76) and *gcy-18* mutants (speed: 291 ± 13 μm/s; p = 0.22; body length: 1.15 ± 0.02 mm; p = 0.86) showed locomotion speeds and body lengths comparable to wild type controls (speed: 252 ± 30 μm/s; body length: 1.14 ± 0.02 mm; Fig. 4–Supplement 2B, C). These results indicate that the loss of context-dependent locomotion modulation is not due to developmental defects or gross impairments in locomotion.”

> *(4) Definition and Baseline Measurements for Locomotion Categories: The finding that tax-4 and kcc-3 contribute to basal locomotion but not to context-dependent locomotion modulation is intriguing. The authors argue that distinct mechanisms regulate these two processes; however, the study does not clearly define the concepts of "basal locomotion" and "context-dependent locomotion," nor does it provide baseline measurements. A clear definition and baseline data are needed to support this conclusion.*

We define basal locomotion as the locomotion speed of worms measured in the binary chamber, where wild-type animals consistently exhibit lower locomotion rates. Measurements from the binary chamber therefore serve as the baseline reference for locomotion speed in our microfluidic assays. Context-dependent locomotion modulation is defined as the quantified difference in locomotion speed between worms in uniform chambers and those in binary chambers. These definitions are now stated in:

Lines 199-201: “We examined the locomotion speed of mutant worms in the binary chambers, which we refer to as the basal speed because wild type worms consistently move slowest in this environment.”

Lines 645-46: “Asterisks above horizontal black lines indicate statistically significant differences in basal speed, defined as speed of worms in the binary chamber”

> ***Recommendations for the authors:***
>
> ***Reviewer #1 (Recommendations for the authors):***
>
> *The availability of strains has not been mentioned. This should be addressed.*

The revised Methods section now includes a complete list of strains used in this study, and we have added a statement indicating that all strains are available upon request.

> *Minor comment:*
>
> *Figure 1C - it should be Idle, not Idel.*

We have corrected the y-axis label in Figure 1C to ‘Idle.’

> ***Reviewer #2 (Recommendations for the authors):***
>
> *This is an interesting and well-written article, which I greatly appreciated reading. There are a few concerns that the authors should address, in my opinion, to provide a more complete and convincing story.*
>
> *Major points:*
>
> *(1) Maybe the material transmitted to me was incomplete, but I did not find the gcy gene screen results. It seems important to present the screen results in full, together with the description of the alleles tested for the 24 gcy genes.*

The revised manuscript now includes the complete results of the *gcy* mutant screen in Figure 2– Supplement 1, with the alleles tested for all 24 *gcy* genes listed in Table S1.

> *(2) I did not find the actual p-values, sample sizes for each condition, or raw data; nor a data availability statement indicating where to retrieve these.*

Statistical significance is indicated by asterisks in all figures, with definitions provided in each figure legend (n.s., $p > 0.05$; *, $p < 0.05$; **, $p < 0.01$; ***, $p < 0.001$). Sample sizes are shown as individual data points in the plots, and we have now added explicit n values to each figure legend for clarity. A Data Availability Statement has also been added to indicate where the raw data can be accessed. Where possible, we have included exact p-values. For analyses using Tukey-Kramer post hoc tests, p-values are reported to four decimal places, reflecting the output limits of the statistical software used.

> *(3) It is not clear why the authors only quantified animal speed for most of the study. What about idle time, turns, and reversals? This choice limits the reach of the study, as we only partly understand what AFD is doing, notably to explain the phenotype in the preference assay.*

Data on idle time, turning frequency, and reversal frequency for wild-type worms are now included in Figure 1F. In addition, we present new data showing that AFD ablation disrupts context-dependent modulation of locomotion speed, idle time, and turning frequency (Figure 4E).

> *(4) Figure 2D and related text: these conclusions are based on a single mutant analysis. Were the millionmutation project lines outcrossed? It would be much more convincing if more gcy alleles were tested (this should be relatively easy since classical alleles are available at the CGC for gcy-8 and gcy-18).*

The million-mutation project lines used in this study were outcrossed prior to analysis. In addition, we confirmed that the observed defects were specifically due to loss of *gcy-18* function by rescuing the phenotype through expression of *gcy-18* cDNA under AFD-specific promoters. This cell-specific rescue shows that the behavioral defects arise from disruption of *gcy-18* rather than from background mutations.

> *(5) It is hard to interpret the speed phenotype when the authors switch between Delta speed and absolute speed display from one figure to another, or even from one panel to another. If only tax-4 and kcc-3 display a constitutive speed phenotype, then there should be no problem showing the absolute speed data in every panel. This is important to convince the reader that major speed changes in mutants are not biasing the interpretation based on Deltas. Indeed, if some mutants move very fast, there might be a ceiling effect. Conversely, if they move very slowly, there might be a 'sickness' effect. Both effects could prevent seeing a tactile-context-dependent modulation, and the results would need to be interpreted much more carefully. Providing the full view on absolute speed levels would also really help support the whole discussion paragraph about the differential regulation of constitutive versus context-dependent locomotion (from L339 onward).*

We focus on Δspeed because it directly quantifies experience-dependent locomotion modulation relative to each strain's own baseline, making it an appropriate metric for comparing tactile plasticity across genotypes. This approach avoids confounding effects from strain-specific differences in overall locomotion levels.

At the same time, we agree that absolute locomotion speed is important to consider when interpreting behavioral phenotypes. To address this, we added plate-based locomotion speed and body length measurements for two key genotypes that lack modulation, *gcy-18* mutants and AFD-ablated worms (Figure 4–Supplement 2B–C). Both exhibit normal locomotion on agar plates, indicating that their defects in tactiledependent modulation are not due to impaired motor ability or general sickness.

In addition, among the mutants tested in microfluidic chambers, *tax-4* mutants display elevated basal speed yet retain robust context-dependent modulation, indicating that ceiling effects do not limit detection of modulation.

> *(6) The gap junction expression is a nice experiment. But there is a major limitation that should be stated: the electrical synapse re-construction is made in a double mutant background in which the whole animal circuitry might be severely affected. It might well be that the restoration of behavioral plasticity represents something totally irrelevant to wild-type nervous system functioning. A cell-specific innexin knockout is needed to fully support the relevance of the AFD-AIB connection.*

We agree that reconstruction of an electrical synapse in an *innexin* double-mutant background carries the limitation that global circuit function may be broadly affected. To address this concern, we performed an additional rescue experiment in a less perturbed genetic background.

As described above, we show that AFD-specific expression of *inx-10* is sufficient to restore tactiledependent locomotion modulation in *inx-10* single mutants (Fig. 6D). This cell-specific rescue does not rely on a double-mutant background and converges on the same outcome as the Cx36-based electrical synapse reconstruction. Together, these complementary approaches support the conclusion that restoring AFD-AIB coupling is sufficient to enable tactile-dependent locomotion modulation, rather than reflecting nonspecific recovery from global circuit disruption.

> *(7) How was developmental age controlled? It seems that all genotypes were grown for a fixed duration (72h). Some mutants, like gcy-8, might grow slower. It would be useful to at least provide control data in wildtype animals showing that behavioral performance is similar even in slightly younger animals (covering the developmental age of the youngest mutant).*

Developmental age was controlled by strict age synchronization and staging criteria rather than growth duration alone. Worms were synchronized by allowing 40-50 young adults to lay eggs on OP50-seeded NGM plates for two hours, after which adults were removed. Developmental stage was further assessed by gonadal morphology, and only young adult animals with 5-10 eggs arranged in a single row were selected for behavioral assays. Using these criteria, all strains, including mutants, consistently reached the assayed stage approximately three days after egg laying, comparable to wild type animals.

To further address the possibility that subtle developmental differences could influence behavior, we measured locomotion speed on agar plates and body length for genotypes that show defects in contextdependent modulation. *gcy-18* mutants and AFD-ablated worms exhibited normal locomotion rates and body size, indicating that their behavioral phenotypes are unlikely to arise from developmental delay or impaired general motor ability. These control data are now included in the revised manuscript (Figure 4– Supplement 2B–C).

> *(8) Plasmid construction description is entirely lacking.*

Description of plasmid construction has been added to the revised Methods.

> *Minor points:*
>
> *(1) 'Context-dependent locomotion' should be replaced by 'tactile context-dependent locomotion' or something similar throughout the manuscript when referring to the impact of the pillar environment.*

Presently, this phrasing shortcut makes the communication too vague throughout, and even confusing when presenting the result of supplementary Figure 2 (where both thermal and tactile contexts are manipulated).

We appreciate this suggestion and have revised the terminology for clarity where appropriate. Prior to introducing the mechanosensory origin of the modulation (that is, before presenting the *mec-10* data), we retain the broader term “context-dependent modulation” to avoid presupposing a tactile mechanism before it is experimentally established.

> *(2) L97: Suggested change along the same lines: "prior experience" -> "prior tactile experience".*

We have made this change as suggested.

> *(3) Figure 1A: Would the author consider swapping the order of conditions displayed in this diagram? It would make more sense to have the same left-to-right order in the whole figure with the binary chamber on the left, particularly since the author describes the results considering the binary chamber as the 'reference point'.*

The order of chambers in Figure 1A has been revised as suggested, with the binary chamber now shown on the left.

> *(4) Figure 1C: 'idel' typo in the axis label.*

The y-axis label has been updated from “idel” to “idle.”

> *(5) Without AFD-specific manipulations, the data with tax-4 and tax-2 mutants provide limited information regarding TAX-4 and TAX-2 role in AFD. It should be explicitly mentioned in the Results section that they might work in other neurons.]*

The revised manuscript now explicitly states that the *tax-2(p694)* allele affects multiple neurons, including BAG, ASE, ADE, and AFD (Lines 421–422).

> *(6) L220-222: The strict meaning of this sentence implies that one attributes a role to AFD in controlling constitutive locomotion, but none of the presented data directly shows this (both kcc-3 and tax-4 mutant phenotypes could arise from additional neurons, regardless of any perturbation in AFD). This should be corrected.*

To avoid implying that AFD directly controls constitutive locomotion, we have removed the sentence in question, "Together, these findings suggest that the role of AFD neurons in modulating context-dependent locomotion is distinct from their thermosensory functions and differs from the mechanisms controlling basal locomotion", from the revised manuscript.

> *(7) L328-329: Overstatement. Without AFD-specific manipulation of TAX-2 and TAX-4, the different mutant phenotypes could be due to different cell types, rather than different protein pairs in the channel heteromers. I would recommend addressing this alternative possibility directly in the discussion, rather than focusing only on one (I agree, very cool) possibility.*

We have clarified this point in the revised text. We now explicitly note that the *tax-2(p694)* mutation affects *tax-2* expression in multiple neurons (AFD, BAG, ASE, and ADE) (Lines 421–422).

> ***Reviewer #3 (Recommendations for the authors):***
>
> *(1) Clarification of inx Gene Expression Analysis (Lines 270-271): The authors should specify how the expression of inx genes in individual neurons was identified.*

The revised manuscript now specifies that innexin expression patterns were identified using the CeNGEN single-cell transcriptomic database (Lines 352–354).

> *(2) Cx36 Expression in AFD and AIB (Lines 287-288): Further clarification is needed on how Cx36 expression was achieved in AFD and AIB.*

We have clarified that Cx36 was expressed specifically in AFD using the *srtx-1b* promoter and in AIB using the *inx-1* promoter, as stated in the main text (Lines 372–373) and the Fig. 6 legend.

https://doi.org/10.7554/eLife.106496.2.sa0